Fluctuations of power injection in randomly driven granular gases.

Paolo Visco,[1,2] Andrea Puglisi,[3] Alain Barrat,[3] Emmanuel Trizac,[2] and Frédéric van Wijland[4,3]

[1] *Laboratoire de Physique Théorique (CNRS UMR 8627), Bâtiment 210, Université Paris-Sud, 91405 Orsay cedex, France*
[2] *Laboratoire de Physique Théorique et Modèles Statistiques (CNRS UMR 8626), Bâtiment 100, Université Paris-Sud, 91405 Orsay cedex, France*
[3] *Laboratoire de Physique Théorique (CNRS UMR8627), Bâtiment 210, Université Paris-Sud, 91405 Orsay cedex, France*
[4] *Laboratoire Matière et Systèmes Complexes (CNRS UMR 7057), Université Denis Diderot (Paris VII), 2 place Jussieu, 75251 Paris cedex 05, France*

(Dated: June 7, 2007)

We investigate the large deviation function $\pi_\infty(w)$ for the fluctuations of the power $\mathcal{W}(t) = wt$, integrated over a time t, injected by a homogeneous random driving into a granular gas, in the infinite time limit. Our analytical study starts from a generalized Liouville equation and exploits a Molecular Chaos-like assumption. We obtain an equation for the generating function of the cumulants $\mu(\lambda)$ which appears as a generalization of the inelastic Boltzmann equation and has a clear physical interpretation. Reasonable assumptions are used to obtain $\mu(\lambda)$ in a closed analytical form. A Legendre transform is sufficient to get the large deviation function $\pi_\infty(w)$. Our main result, apart from an estimate of all the cumulants of $\mathcal{W}(t)$ at large times t, is that $\pi_\infty(w)$ has no negative branch. This immediately results in the failure of the Gallavotti-Cohen Fluctuation Relation (GCFR), that in previous studies had been suggested to be valid for injected power in driven granular gases. We also present numerical results, in order to discuss the finite time behavior of the fluctuations of $\mathcal{W}(t)$. We discover that their probability density function converges extremely slowly to its asymptotic scaling form: the third cumulant saturates after a characteristic time τ larger than ~ 50 mean free times and the higher order cumulants evolve even slower. The asymptotic value is in good agreement with our theory. Remarkably, a numerical check of the GCFR is feasible only at small times (at most $\tau/10$), since negative events disappear at larger times. At such small times this check leads to the misleading conclusion that GCFR is satisfied for $\pi_\infty(w)$. We offer an explanation for this remarkable apparent verification. In the inelastic Maxwell model, where a better statistics can be achieved, we are able to numerically observe the failure of GCFR.

PACS numbers:

I. INTRODUCTION

In non-equilibrium statistical physics few general results have been established [1]. A quick historical survey begins with the Einstein relation [2] between the velocity fluctuations at equilibrium of a Brownian particle and the variation of its velocity under the effect of a small applied force. This relation between fluctuations and dissipation has been then explored and fruitfully extended in many ways, first by Onsager [3], and then by Green [4] and Kubo [5]. All those works have been concluded with the establishment of the Green-Kubo formulae and the fluctuation-dissipation theorem, essentially a local formulation of the previous relations. Later, a thermodynamical phenomenological description [6] was formulated, based on the hypothesis of local thermal equilibrium. Within the latter framework the entropy variations of a macroscopic system evolve according to the evolution equation

$$\frac{\mathrm{d}S}{\mathrm{d}t} = \sigma - \int_{\text{system}} \mathrm{d}V \nabla \cdot \mathbf{J}_S \quad . \tag{1}$$

The first term σ is the irreversible entropy source, which vanishes at equilibrium, and is strictly positive out of thermal equilibrium. The second term $\int \nabla \cdot \mathbf{J}_S$ is related to the external constraints (or fields), which are necessary to drive the system in a non-equilibrium state. In a steady state, of course those two terms are equal. Furthermore, as opposed to σ, whose origin is purely statistical, $\mathbf{J}_S$ is the average of a microscopically well defined quantity. We shall refer to this quantity as a mean entropy flux. In many physical systems this entropy flux is associated to a current, where the conveyed quantities are usually the energy, the momentum, or the density.

More recently, attempts to reveal the general behavior of large classes of systems have been performed, focusing on large deviation properties and on macroscopic quantities. For a long time the study of dissipative systems has been centered on local quantities, such as structure factors, correlations, and velocity fields. Nevertheless recent results [7] support the intuition that in order to observe universal features, it is helpful to study "global" quantities. Averaging is indeed an effective way to bypass differences arising from microscopic details, keeping however essential features.

Most spectacular and surprising examples are provided in [7, 8], where it turns out that three different quantities (the total magnetization of the two-dimensional XY model near the critical point, the instantaneous injected power in a turbulent flow, and the energy fluctuations of a cooling granular gas close to the clustering instability), suitably rescaled, display the same probability distribution function (pdf).

In addition, we have learnt from equilibrium statistical mechanics that the most useful informations are contained in the state functions, the free energy being the main example. Those functions are, in the probabilistic interpretation, large deviation functions (ldf)[1]. In equilibrium statistical physics, the large deviation principle enters when considering microscopic quantities summed over all the degrees of freedom, or integrated over the whole volume of the system. Thus, large deviations are associated to the size-extensivity of the macroscopic quantities of interest. As a matter of fact in non-equilibrium systems the dynamics, and hence the time, plays a central role (even in stationary states). This has led to the introduction of time extensive quantities, which can be easily obtained integrating a stationary quantity over a given time interval. The simplest choice to attempt for a universal description seems indeed to study the time large deviation function of a flux integrated over a time t. In this framework the infinite time limit could be seen as the "non-equilibrium counterpart" of the thermodynamic limit in equilibrium physics.

With this objective Evans, Cohen and Morriss discovered a particular symmetry property of the ldf of the integrated injected power for a system of thermostatted sheared hard disks [9]. In order to have a non-equilibrium steady state, it is necessary to have a competition between at least two forces acting on the system. In the particular case of [9] the energy injected by the shearing force is compensated by an external thermostatting force, created *ad hoc*, in such a way that the total kinetic energy of the system is constant. This symmetry property has subsequently been formalized in a theorem by Gallavotti and Cohen [10]. The theorem has been proved for deterministic and time reversible dynamical systems, under the hypothesis of strong chaoticity. In this context the quantity $\mathcal{S}(t)$ is the phase space contraction rate integrated over a time t. It turns out that in a large class of dynamical systems the phase space contraction rate is endowed with the significance of the entropy flux defined in non-equilibrium thermodynamics. For thermostatted systems [11] this is equivalent to the power injected by the thermostatting force divided by the temperature of the system [9, 10]. The Gallavotti-Cohen Fluctuation Relation (GCFR from now on) concerns the large deviation function of the probability $P(\mathcal{S},t)$ of a quantity playing the role of the entropy flux, defined as

$$\pi_\infty(s) = \lim_{t\to\infty} \pi_t(s), \quad \text{with} \quad \pi_t(s) = \frac{1}{t}\log P(st,t)\,. \tag{2}$$

Then, the GCFR reads:

$$\pi_\infty(s) - \pi_\infty(-s) = s \ . \tag{3}$$

Similar results were obtained for Markov processes by Kurchan [12] and by Lebowitz and Spohn [13].

After the GCFR has been proposed, several attempts of verification in experiments and numerical simulations have been proposed, always with success [14]. In many of these attempts however, the quantity $\mathcal{S}(t)$ was not the integrated phase space contraction rate, and the original hypothesis of the theorem were not guaranteed. The phase space contraction rate is indeed usually not accessible in experiments, and strong chaoticity (Anosov property) is not strictly satisfied in most real systems. The choice of the quantity $\mathcal{S}(t)$ usually goes to functionals that are related to equilibrium or near-equilibrium entropy-like quantities. Typically one expects that the fluxes defined in non-equilibrium thermodynamics [6] are the macroscopic analogous of the phase space contraction rate, and this is definitely true in specific thermostatted models [11]. The rate of heat transport from the thermostat, or equivalently the power injected by the thermostat into the system, divided by the temperature of the thermostat, is the natural candidate. In order to check for possible extensions of the GCFR for systems without time-reversal invariance the study of the pdf of the injected power seems the simplest choice. Such a program has been initiated by Aumaître *et al.* [15], who measured the injected power distribution for several microscopically irreversible systems. Within the available accuracy, they concluded that the GCFR holds but importantly pointed out the possible relevance of spurious effects at large times where the necessarily limited data gathered may not allow to sample the regions where GCFR violations could exist. An analytical approach was also proposed by Farago [16], who analytically computed the ldf of a particular model without time-reversal symmetry, showing that GCFR does not hold, at least for this particular model. Nevertheless a recent experiment [17] observed the validity of the GCFR measuring the integrated injected power rendered dimensionless by an appropriate energy scale.

---

[1] As an example, for a system in the canonical ensemble with a free energy $F(T,V,N)$ and a partition function $Z = \mathrm{e}^{-\beta F}$, all the physical features (such phase transitions, *etc.*) are contained in the free energy per particle $f = F/N$, which in the thermodynamic limit is $f = -\frac{1}{\beta}\lim_{N\to\infty}\frac{\log Z}{N}$, which only depends on intensive variables.

In a recent study, we have shown that in general the GCFR is not satisfied for the integrated injected power in homogeneously driven granular gases [18] and that the results of the experiment described in [17] were insufficient to claim its verification [19]. In this paper we discuss the derivation of an equation for the large deviation function for injected power in homogeneously driven granular gases, obtaining its solution under a series of reasonable approximations. The Gallavotti-Cohen Fluctuation Relation cannot be satisfied in this model because the injected power large deviation has no negative tail. We also provide details from numerical simulations of the model, showing how the GCFR may seem to be satisfied at small times [i.e. considering $\pi_t(s)$ instead of $\pi_\infty(s)$] and small values of s. In experiments and simulations true large deviations are argued to be unreachable.

In our approach, the granular gas is modeled as a dilute system of inelastic hard spheres. The heating mechanism that allows the gas to reach a steady-state is the widely used stochastic thermostat [20]. It differs from the experimental setup of Ref. [17] in that the energy injection is fully uniform (each particle is subjected to a random force) instead of being boundary driven. The model under study is however relevant for other two dimensional experimental situations, see e.g. [21]. Our goal is to compute, analytically and numerically, the distribution of the power injected into the gas by those random kicks.

In section II the inelastic Hard Spheres model is presented and the details of the derivation of the large deviation function of the injected power are presented. Section III repeats the procedure for the closely related and much more tractable inelastic Maxwell Model (practical motivations will become clear later). Numerical results are provided in section IV. We then conclude the paper (Section V) with a discussion of our results.

II. THE INELASTIC HARD SPHERES MODEL

A. The Model

We consider a granular gas made up of N identical spherical particles undergoing dissipative collisions. The collisions between two particles i and j conserve the total momentum and reduce the normal component of the relative velocity, i.e. $(\mathbf{v}_i^* - \mathbf{v}_j^*)\cdot\hat{\boldsymbol{\sigma}} = -\alpha(\mathbf{v}_i - \mathbf{v}_j)\cdot\hat{\boldsymbol{\sigma}}$, where the stars denote the post-collisional velocities and $\hat{\boldsymbol{\sigma}}$ the direction joining the centers of the colliding particles. Energy injection, achieved by means of random forces (kicks) acting independently on each particle, drives the gas into a non-equilibrium steady state. The equation of motion governing the dynamics of each particle is therefore:

$$\frac{\mathrm{d}\mathbf{v}_i}{\mathrm{d}t} = \mathbf{F}_i^{\mathrm{coll}} + \mathbf{F}_i^{\mathrm{th}}, \tag{4}$$

where $\mathbf{F}_i^{\mathrm{coll}}$ is the force due to collisions and $\mathbf{F}_i^{\mathrm{th}}$ is a Gaussian white noise (i.e. $\langle F_{i\gamma}^{\mathrm{th}}(t) F_{j\delta}^{\mathrm{th}}(t')\rangle = 2\Gamma\delta_{ij}\delta_{\gamma\delta}\delta(t-t')$, where the angular brackets denote statistical average; the subscripts i and j are used to refer to the particles, while γ and δ denote the Euclidean components of the random force). This model is one of the most studied in granular gas theory and reproduces many qualitative features of real driven inelastic gases [20, 22]. After a few collisions per particle, the system attains a non-equilibrium stationary state. Furthermore, this state is homogeneous and does not develop spatial inhomogeneities, in contrast to what happens for example in the freely cooling state of a granular gas. From the equations of motion it is possible to derive the Boltzmann equation governing the evolution of the one-particle velocity distribution function f which, since the system is homogeneous, will not depend on the positions of the particles. If, in addition, we resort to the molecular chaos assumption, this Boltzmann equation reads [22]:

$$\partial_t f(\mathbf{v}_1, t) = J[f, f] + \Gamma\Delta_{\mathbf{v}_1} f(\mathbf{v}_1)\ , \tag{5}$$

where the Laplace operator $\Delta_{\mathbf{v}} \equiv (\partial/\partial_{\mathbf{v}})^2$ is a diffusion term in velocity space characterizing the effect of the random force, while $J[f, f]$ is the collision integral, which takes into account the inelasticity of the collisions:

$$J[f,f] = \frac{1}{\ell}\int \mathrm{d}\mathbf{v}_2 \int' \mathrm{d}\hat{\boldsymbol{\sigma}}(\mathbf{v}_{12}\cdot\hat{\boldsymbol{\sigma}})\left(\frac{1}{\alpha^2} f(\mathbf{v}_1^{**}) f(\mathbf{v}_2^{**}) - f(\mathbf{v}_1) f(\mathbf{v}_2)\right)\ . \tag{6}$$

In the above expression of the collision integral the notation $\mathbf{v}_{12}$ denotes the relative velocity between particles 1 and 2, while the two stars superscript (i.e. $\mathbf{v}^{**}$) denotes the pre-collisional velocity of a particle having velocity $\mathbf{v}$. Moreover the length $\ell = (n\sigma^{d-1})^{-1}$, where n is the particle density, σ the diameter of the particles and d the space dimension, is proportional to the mean free path. Finally, the primed integral $\int'$ will be used as a short-hand notation to denote $\int \Theta(\mathbf{v}_{12}\cdot\hat{\boldsymbol{\sigma}})$, where Θ is the Heaviside step function. The granular temperature of the system is defined as the mean kinetic energy per degree of freedom, $T_g = \langle v^2\rangle/d$. Such a definition for the temperature is purely kinetic, and can *a priori* not be interpreted as a thermodynamical temperature.

B. The velocity distribution function

In this section we briefly review the known results concerning the solution of the Boltzmann equation (5). The stationary solution of this equation has extensively been investigated in the last years, but an exact solution is still missing. Nevertheless a general method is to look for solutions in the form of a Gaussian distribution multiplied by a series of Sonine polynomials:

$$f_{st}(\mathbf{v}) = e^{-\frac{v^2}{2T_g}} \left(1 + \sum_{p=1}^{\infty} a_p S_p\left(\frac{v^2}{2T_g}\right)\right) \ . \tag{7}$$

The expression of the first three Sonine polynomials is:

$$\begin{aligned} S_0(x) &= 1 \\ S_1(x) &= -x + \frac{1}{2}d \\ S_2(x) &= \frac{1}{2}x^2 - \frac{1}{2}(d+2)x + \frac{1}{8}d(d+2) \ . \end{aligned} \tag{8}$$

Moreover the coefficients a_p are found to be proportional to the averaged polynomial of order p:

$$a_p = A_p \left\langle S_p\left(\frac{v^2}{2T_g}\right)\right\rangle \ , \tag{9}$$

where A_p is a constant. From this observation one directly obtains that the first coefficient a_1 vanishes by definition of the temperature. A first approximation for the velocity pdf is therefore to truncate the expansion at second order ($p = 2$). An approximated expression for the coefficient a_2 has been found as a function of the restitution coefficient α and the dimension d [22, 23, 24]. It must be noted that this approximation is only valid for not too large velocities, since the tails of the pdf have been shown [22] to be overpopulated with respect to the Gaussian distribution. It is known [22] that at high energies $\log f(\mathbf{v}) \sim -(v/v_c)^{3/2}$ with a threshold velocity v_c that diverges when the dimension d goes to infinity. This means that at high dimensions the distribution is almost a Gaussian with small Sonine corrections. All the above results have been confirmed by numerical simulations, in particular through Molecular Dynamics (MD) and Direct Simulation Monte Carlo (DSMC) [25] methods. Those two numerical methods, although very different, show a surprisingly good agreement. This points out the validity of the molecular chaos assumption and thus the relevance of the DSMC method, which is particularly well adapted to simulate the dynamics of a homogeneous dilute gas.

C. Equation for the injected power

In this section, we will show how to obtain a kinetic equation able to describe the behavior of the pdf of the integrated injected power at large times. The latter quantity is the total work $\mathcal{W}$ provided by the thermostat over a time interval $[0, t]$:

$$\mathcal{W}(t) = \int_0^t \mathrm{d}t \sum_i \mathbf{F}_i^{th} \cdot \mathbf{v}_i \, . \tag{10}$$

Our interest goes to the distribution of $\mathcal{W}(t)$, denoted by $P(\mathcal{W}, t)$, and to its associated large deviation function $\pi_\infty(w)$ defined for the reduced variable $w = \mathcal{W}/t$ ($\mathcal{W}(t)$ being extensive in time):

$$\pi_\infty(w) = \lim_{t\to\infty} \pi_t(w) \ \ , \pi_t(w) = \frac{1}{t} \ln P(\mathcal{W} = wt, t) \, . \tag{11}$$

We introduce $\rho(\Gamma_N, \mathcal{W}, t)$, the probability that the system is in state Γ_N at time t with $\mathcal{W}(t) = \mathcal{W}$. The function we want to calculate is

$$P(\mathcal{W}, t) = \int \mathrm{d}\Gamma_N \rho(\Gamma_N, \mathcal{W}, t) \ \ . \tag{12}$$

We shall focus on the generating function of the phase space density

$$\hat{\rho}(\Gamma_N, \lambda, t) = \int \mathrm{d}\mathcal{W} \mathrm{e}^{-\lambda \mathcal{W}} \rho(\Gamma_N, \mathcal{W}, t) \tag{13}$$

and on the large deviation function of

$$\hat{P}(\lambda,t)=\int \mathrm{d}\mathcal{W}\mathrm{e}^{-\lambda\mathcal{W}}P(\mathcal{W},t)=\int \mathrm{d}\Gamma_N\hat{\rho}(\Gamma_N,\lambda,t) \quad , \tag{14}$$

which we define as

$$\mu(\lambda)=\lim_{t\to\infty}\frac{1}{t}\ln\hat{P}(\lambda,t) \ . \tag{15}$$

Note that $\mu(\lambda)$ is the generating function of the cumulants of $\mathcal{W}$, namely

$$\lim_{t\to\infty}\frac{\langle\mathcal{W}^n\rangle_c}{t}=(-1)^n\left.\frac{\mathrm{d}^n\mu(\lambda)}{\mathrm{d}\lambda^n}\right|_{\lambda=0} \quad . \tag{16}$$

Moreover $\pi_\infty(w)$ can be obtained from $\mu(\lambda)$ by means of a Legendre transform, i.e. $\pi_\infty(w)=\mu(\lambda_*)+\lambda_* w$ with λ_* such that $\mu'(\lambda_*)=-w$.

The observable $\mathcal{W}$ is non-stationary and we are interested in the evolution equation for the extended phase space density $\rho(\Gamma_N,\mathcal{W},t)$. It varies in time under the combined effect of the inelastic collisions (which do not trigger any change in $\mathcal{W}$) and of the random kicks:

$$\partial_t\rho=\left.\partial_t\rho\right|_{\text{collisions}}+\left.\partial_t\rho\right|_{\text{kicks}} \tag{17}$$

Instantaneous collisions do not modify the value of $\mathcal{W}$, only the random kicks will affect it. In between two successive collisions, the amount of energy provided by the thermostat on each particle is $\Delta\mathcal{W}=(v(t_{i+1}^-)^2-v(t_i^+)^2)/2$, where t_i denotes the time of the $i-$th collision and the $-$ $(+)$ superscript simply denotes that the value of the velocity at a collision time has to be taken before (after) the collision has taken place.

In order to characterize the role of the thermostat on the generating function $\hat{\rho}$ it is useful to discretize the problem in velocity space, considering that the effect of the random kicks on one particle is a continuous time random walk of its velocity on a d dimensional lattice of step a, with hopping rate γ. It then appears that the observable $\mathcal{W}$ is Markovian, and the master equation governing the evolution of the probability of being at site $\mathbf{n}$ (which represents the discretized velocity of one particle) at time t, with the value $\mathcal{W}(t)=\mathbf{n}(t)^2/2$ reads:

$$\partial_t P(\mathbf{n},\mathcal{W},t)=\gamma\sum_{\mathbf{a}}\left(P(\mathbf{n}+\mathbf{a},\mathcal{W}+\mathbf{n}\cdot\mathbf{a}+a^2/2,t)+P(\mathbf{n}-\mathbf{a},\mathcal{W}-\mathbf{n}\cdot\mathbf{a}+a^2/2,t)\right)-2d\gamma P(\mathbf{n},\mathcal{W},t) \ . \tag{18}$$

Here $\{\mathbf{a}\}$ is a set of d orthogonal vectors defining the lattice. This yields, in terms of the generating function $\hat{P}(\mathbf{n},\lambda',t)=\int \mathrm{d}\mathcal{W}\mathrm{e}^{-\lambda'\mathcal{W}}P(\mathbf{n},\mathcal{W},t)$,

$$\partial_t\hat{P}(\mathbf{n},\lambda',t)=\gamma\sum_{\mathbf{a}}\left(\hat{P}(\mathbf{n}+\mathbf{a},\lambda',t)\mathrm{e}^{\lambda'\mathbf{n}\cdot\mathbf{a}+\lambda' a^2/2}+\hat{P}(\mathbf{n}-\mathbf{a},\lambda',t)\mathrm{e}^{-\lambda'\mathbf{n}\cdot\mathbf{a}+\lambda' a^2/2}\right)-2d\gamma\hat{P}(\mathbf{n},\lambda',t). \tag{19}$$

Next, it is possible to expand the above expression in powers of a at order a^2 and consider the continuum limit $a\to 0$ with the scaling variables $\mathbf{v}=\mathbf{n}\,a$, $\Gamma=\gamma a^2$ and $\lambda=\lambda'/a$ fixed. Finally this yields, considering that the thermostat acts independently on each particle,

$$\left.\partial_t\hat{\rho}\right|_{\text{kicks}}=\sum_i\left[\Gamma(\Delta_{\mathbf{v}_i}+2\lambda\Gamma\mathbf{v}_i\cdot\partial_{\mathbf{v}_i}+\Gamma(d\lambda+\lambda^2 v_i^2)\right]\hat{\rho} \tag{20}$$

This additional piece is linear in $\hat{\rho}$, just as the collision part. The large time behavior of $\hat{\rho}$ is thus governed by the largest eigenvalue $\mu(\lambda)$ of the evolution operator of $\hat{\rho}$. In the large time limit, we expect that

$$\hat{\rho}(\Gamma_N,\lambda,t)\simeq C(\lambda)\mathrm{e}^{\mu(\lambda)t}\tilde{\rho}(\Gamma_N,\lambda), \tag{21}$$

where $C(\lambda)=1/\int \mathrm{d}\Gamma_N\tilde{\rho}(\Gamma_N,\lambda)$, and $\tilde{\rho}(\Gamma_N,\lambda)$ is the eigenfunction associated to μ, which for convenience has been taken normalized to unity (in order that $C(\lambda)\neq 0$ the initial state must have a nonzero projection onto this eigenfunction). We then introduce

$$\hat{f}^{(1)}(\mathbf{v},\lambda,t)=\int \mathrm{d}\Gamma_{N-1}\hat{\rho}, \tag{22}$$

where $\int \mathrm{d}\Gamma_{N-1}$ means an integration over $N-1$ particle coordinates. This function obeys

$$\partial_t \hat{f}^{(1)}(\mathbf{v},\lambda,t) = \Gamma\Delta_{\mathbf{v}}\hat{f}^{(1)} + 2\lambda\Gamma\partial_{\mathbf{v}}\cdot\mathbf{v}\hat{f}^{(1)} + \Gamma(\lambda^2 v^2 - d\lambda)\hat{f}^{(1)} + \hat{J} \tag{23}$$

with $\hat{J} = \int \mathrm{d}\mathcal{W}\mathrm{e}^{-\lambda\mathcal{W}}J$ the Laplace transform of the collision integral J in which the usual velocity distributions $f^{(1)}(\mathbf{v}_1,t)$ and $f^{(2)}(\mathbf{v}_1,\mathbf{v}_2,t)$ are replaced by $f^{(1)}(\mathbf{v},\mathcal{W},t)$ and $f^{(2)}(\mathbf{v}_1,\mathbf{v}_2,\mathcal{W},t)$ involving $\mathcal{W}$ as well as the velocities. Quite unexpectedly the above equation has a clear physical interpretation: consider a many particle system where a noise of strength Γ and a viscous friction-like force $\mathbf{F} = -2\lambda\Gamma\mathbf{v}$ act independently on each particle, and where the particles interact by inelastic collisions. Consider then that the particles annihilate/branch (depending on the sign of λ) at constant rate $d\lambda\Gamma$, and branch with a rate proportional to $\lambda^2 v^2\Gamma$. Then, the equation governing the evolution of the one particle velocity distribution of such a system is exactly the equation (23), where λ is a parameter tuning the strength of the external fields. In spite of there being no *a priori* reason for that, $\tilde{\rho}$, as well as $\tilde{f}^{(1)} = \int \mathrm{d}\Gamma_{N-1}\tilde{\rho}$, can consequently be interpreted as probability density functions.

Since $\hat{\rho}(\Gamma_N,\lambda,t) \simeq C(\lambda)\mathrm{e}^{\mu(\lambda)t}\tilde{\rho}(\Gamma_N,\lambda)$, the one and two-point functions $f^{(1)}(\mathbf{v},\mathcal{W},t)$ and $f^{(2)}(\mathbf{v}_1,\mathbf{v}_2,\mathcal{W},t)$ that enter the expression of J are expected to verify in $\lambda-$space, at large times,

$$\hat{f}^{(1)}(\mathbf{v}_1,\lambda,t) = C(\lambda)\mathrm{e}^{\mu t}\tilde{f}^{(1)}(\mathbf{v}_1,\lambda), \tag{24}$$

and

$$\hat{f}^{(2)}(\mathbf{v}_1,\mathbf{v}_2,\lambda,t) = C(\lambda)\mathrm{e}^{\mu t}\tilde{f}^{(2)}(\mathbf{v}_1,\mathbf{v}_2,\lambda), \tag{25}$$

where both $\tilde{f}^{(1)} = \int \mathrm{d}\Gamma_{N-1}\tilde{\rho}$ and $\tilde{f}^{(2)} = \int \mathrm{d}\Gamma_{N-2}\tilde{\rho}$ are normalized to unity. We perform the following molecular-chaos-like assumption:

$$\tilde{f}^{(2)}(\mathbf{v}_1,\mathbf{v}_2,\lambda) \simeq \tilde{f}^{(1)}(\mathbf{v}_1,\lambda)\tilde{f}^{(1)}(\mathbf{v}_2,\lambda) \tag{26}$$

which does have a definite physical interpretation in the language of the inelastic hard-spheres with fictitious dynamics (viscous friction, velocity dependent branching/annihilation) described in the above paragraph. Then we get that

$$\begin{aligned}\mu\tilde{f}(\mathbf{v},\lambda,t) =& \Gamma\Delta_{\mathbf{v}}\tilde{f} + 2\lambda\Gamma\mathbf{v}\cdot\partial_{\mathbf{v}}\tilde{f} + \Gamma(d\lambda+\lambda^2v^2)\tilde{f} \\ &+ \frac{1}{\ell}\int_{\mathbf{v}_{12}\cdot\hat{\boldsymbol{\sigma}}>0}\mathrm{d}\mathbf{v}_2\mathrm{d}\hat{\boldsymbol{\sigma}}\,\mathbf{v}_{12}\cdot\hat{\boldsymbol{\sigma}}\left[\alpha^{-2}\tilde{f}(\mathbf{v}_1^{**},\lambda)\tilde{f}(\mathbf{v}_2^{**},\lambda) - \tilde{f}(\mathbf{v}_1,\lambda)\tilde{f}(\mathbf{v}_2,\lambda)\right]\end{aligned} \tag{27}$$

where we have now omitted the superscript (1) denoting the one-point function. Note that the truncation (26) respects two physical requirements. First, it does conserve $\mathcal{W}$ throughout a collision. This can be observed rewriting the product of the two one-point functions as

$$\tilde{f}\left(\mathbf{v}_1^{(**)},\lambda\right)\tilde{f}\left(\mathbf{v}_2^{(**)},\lambda\right) = \int \mathrm{d}\mathcal{W}\,\mathrm{d}\mathcal{W}_1\,\mathrm{d}\mathcal{W}_2\,\delta(\mathcal{W}_1+\mathcal{W}_2-\mathcal{W})\mathrm{e}^{-\lambda\mathcal{W}}g\left(\mathbf{v}_1^{(**)},\mathcal{W}_1\right)g\left(\mathbf{v}_2^{(**)},\mathcal{W}_2\right)\ , \tag{28}$$

where $g(\mathbf{v},\mathcal{W}) = \int \mathrm{d}\Gamma_{N-1}\,\rho(\Gamma_N,\mathcal{W})$. This leads to the simple remark that if the particle 1 carries a fraction $\mathcal{W}_1$ of the integrated injected power before a collision, and the particle 2 carries a fraction $\mathcal{W}_2$, then the global amount $\mathcal{W} = \mathcal{W}_1 + \mathcal{W}_2$ is preserved in a collision. Second, the $\lambda = 0$ limiting case yields the usual Boltzmann equation, since in this case a stationary solution exists, and hence $\mu(\lambda=0) = 0$. The boundary condition to the evolution equation above is thus:

$$\tilde{f}(\mathbf{v},\lambda=0) = f_{st}(\mathbf{v}) \tag{29}$$

with $f_{st}(\mathbf{v})$ the stationary velocity pdf (cf. Eq.(7)).

D. The limits for large velocity and for $\lambda \to \infty$.

Equation (27) can be written in the form:

$$\mu\tilde{f}(\mathbf{v}_1,\lambda) = \Gamma\mathrm{e}^{-\frac{\lambda v^2}{2}}\Delta_{\mathbf{v}_1}\left(\mathrm{e}^{\frac{\lambda v_1^2}{2}}\tilde{f}(\mathbf{v}_1,\lambda)\right) + \hat{J}(\tilde{f},\tilde{f})\ . \tag{30}$$

Defining a new function $F(\mathbf{v},\lambda)=\exp\left(\frac{\lambda v^2}{2}\right)\tilde{f}(\mathbf{v},\lambda)$ the above equation reads:

$$\mu(\lambda)F(\mathbf{v}_1,\lambda)=\Delta_{\mathbf{v}_1}F(\mathbf{v}_1,\lambda)+J_\lambda[F,F]\ , \tag{31}$$

where

$$J_\lambda[F,F]=\int \mathrm{d}\mathbf{v}_2\int' \mathrm{d}\hat{\boldsymbol{\sigma}}\,(\mathbf{v}_{12}\cdot\hat{\boldsymbol{\sigma}})\,\mathrm{e}^{-\frac{\lambda v_2^2}{2}}\left(\frac{1}{\alpha^2}\mathrm{e}^{-\frac{\lambda}{4}\left(\frac{1}{\alpha^2}-1\right)(\mathbf{v}_{12}\cdot\hat{\boldsymbol{\sigma}})^2}F(\mathbf{v}_1^{**},\lambda)F(\mathbf{v}_2^{**},\lambda)-F(\mathbf{v}_1,\lambda)F(\mathbf{v}_2,\lambda)\right) \tag{32}$$

is the collision integral. Repeating the arguments by van Noije and Ernst [22] we shall now compute the behavior of the tails of $\tilde{f}$. In the large velocities limit one has $v_{12}\sim v_1$, and for $\lambda>0$ the gain term of the collision integral can be neglected, since the argument of its exponential prefactor is strictly negative for inelastic collisions ($\alpha<1$). In this limit the solution of eq.(31) is of the form:

$$\log\tilde{f}(\mathbf{v},\lambda)=-\lambda\frac{v^2}{2}-\frac{2}{3}\sqrt{\frac{\beta_1}{\ell\Gamma}}v^{3/2}-\frac{\mu}{\Gamma}\sqrt{\frac{\ell\Gamma}{\beta_1}}v^{1/2}+o(v^{1/2})\ , \tag{33}$$

where $\beta_1=\pi^{(d-1)/2}/\Gamma((d+1)/2)$ comes from an angular integration. This result is important since it shows that the high velocity tails of the function $\tilde{f}(\mathbf{v},\lambda)$ are Gaussian. For $\lambda=0$ the known result concerning the non-Gaussian tails of the one-particle velocity pdf [22] is recovered.

Moreover, in the limit $\lambda\to\infty$ the gain term of the collision integral can be neglected. Thus, the resulting equation can be interpreted as a Boltzmann equation for a system of particles subjected to a random force, interacting with an "effective potential" which makes the collision kernel $\propto(\mathbf{v}_{12}\cdot\hat{\boldsymbol{\sigma}})\exp-\lambda v_2^2/2$, and annihilating when a collision occurs. The Boltzmann equation of this system reads:

$$\partial_t F=\Delta_{\mathbf{v}}F-\int \mathrm{d}\mathbf{v}_2\int' \mathrm{d}\hat{\boldsymbol{\sigma}}(\mathbf{v}_{12}\cdot\hat{\boldsymbol{\sigma}})e^{-\frac{\lambda v_2^2}{2}}F(\mathbf{v}_1)F(\mathbf{v}_2)\ . \tag{34}$$

This immediately shows that $\mu(\lambda)$ for high values of λ is always negative, since the density of particles (given by the integral of F) is clearly decreasing. The consequence of this observation, together with the fact that $\mu(\lambda)$ must be always convex and is zero in $\lambda=0$, is that $\mu'(\lambda)<0$ for any value of λ . For negative w, there is therefore no possible λ_* satisfying $\mu'(\lambda_*)=-w$: the immediate consequence is that $\pi_\infty(w)$, i.e. the Legendre transform of $\mu(\lambda)$, is not defined for negative w. As announced in the introduction, this is a key point in invalidating the GCFR.

E. Energy balance

Before going further in the analytical calculation of $\pi_\infty(w)$, we provide a complementary argument for the absence of negative tail. The reasoning takes as starting point the fact that the energy variations in a time t are given by the difference of the injected power integrated over a time t, $\mathcal{W}(t)$, and the energy dissipated through collisions over the same time interval $\mathcal{D}(t)$. Hence the fluctuating total kinetic energy $E(t)=\sum_i \mathbf{v}_i^2/2$ varies according to

$$\Delta E(t)=E(t)-E(0)=\mathcal{W}(t)-\mathcal{D}(t)\ , \tag{35}$$

where $\mathcal{D}\geq 0$. It is important to note that the above equation is very general, and applies to many dissipative systems where an external driving supplies the energy lost by some dissipation mechanism in order to reach a non-equilibrium steady state. Let us define the probability $\mathcal{P}(z)$ of having $\Delta E(t)=z$. If the total work $\mathcal{W}(t)$ is sampled starting from a fixed initial condition $E(0)=const$, then it is easy to show that the left tail of the distribution $\mathcal{P}$ is bounded by $-E(0)$ (since $E(t)\geq 0$). This implies that the large deviation function associated to the stationary quantity $\Delta E(t)$ has no negative contributions, as well as the large deviation function π_∞ of the total work $\mathcal{W}=\mathcal{D}+\Delta E$, since it is the sum of two quantities with no large negative events in the long times limit. On the contrary, if the total work distribution is obtained sampling over segments of a unique trajectory, the above argument does not hold anymore, since both $E(t)$ and $E(0)$ are fluctuating quantities. Thus, the pdf $\mathcal{P}(z)$ is no more bounded, but, for times much longer than the characteristic energy correlation time, it is symmetric with respect to the $z=0$ axis. Our purpose in this section is to give some phenomenological arguments to understand under which conditions on $\mathcal{P}(z)$ it is likely that $\mathcal{W}$ and $\mathcal{D}$ have the same large deviations function. Since ΔE is not a time-extensive variable, in principle it does not have large deviations. Nevertheless a large fluctuation of ΔE may affect the behavior of the time-extensive

quantities $\mathcal{W}$ or $\mathcal{D}$. Hence we will focus our attention to the tails of ΔE, which we will suppose to have a stretched exponential behavior with an exponent δ (i.e. $\mathcal{P}(z) \sim \exp -|z|^\delta$ when $z \to \pm\infty$). It is useful then to note that

$$\zeta(\epsilon) = \lim_{t\to\infty} \frac{1}{t} \log \mathcal{P}(\Delta E = \epsilon t) = \begin{cases} 0 \ , & \text{if } \delta < 1 \\ -|\epsilon| \ , & \text{if } \delta = 1 \\ -\infty \ , & \text{if } \delta > 1 \text{ (and } \epsilon \neq 0). \end{cases} \tag{36}$$

We therefore observe that the exponential distribution ($\delta = 1$) plays a limiting role for the function ζ. Besides, if one looks at what happens in Laplace space (i.e. to the large deviation function of the Laplace transform of $\mathcal{P}$), the infinite time limit does not depend anymore on the particular value of the exponent δ:

$$\vartheta(\lambda) = \lim_{t\to\infty} \frac{1}{t} \log\langle \mathrm{e}^{\lambda \Delta E}\rangle = 0 \ . \tag{37}$$

Now a natural question arise: is it possible to recover the function ζ knowing ϑ ? Usually the Legendre transform is the link between those two functions. It is easy to see that the Legendre transform of $\vartheta = 0$ gives $\zeta = -\infty$, independently of δ. As we will show, this "failure" of the Legendre transform is related with analyticity breaking of the function ϑ. If $\delta > 1$ the Laplace transform of $\mathcal{P}$ is analytical in the whole complex plane of λ. On the contrary, if $\delta = 1$, the Laplace transform of $\mathcal{P}$ is very likely to presents singularities, as well as analytical cuts in the complex plane of λ. The Legendre transform as an inversion formula of the Laplace transform is obtained using the saddle point method when integrating the inverse Laplace integral on a straight line parallel to the imaginary axis of the complex λ plane. It is seen indeed that if $\langle \exp \lambda \Delta E\rangle$ presents singularities or cuts, then the Laplace transform cannot be inverted anymore.

Returning to our original problem, it now seems reasonable to argue that in a general way the large deviations functions associated to the Laplace transform of the pdf of $\mathcal{W}$ and $\mathcal{D}$ are the same (i.e. $\lim\langle\exp(-\lambda\mathcal{W})\rangle/t = \lim\langle\exp(-\lambda\mathcal{D})\rangle/t$). However, if $\mathcal{P}(\Delta E)$ has exponential tails, non-analyticities may arise in Laplace space, and the large deviations functions of $\mathcal{W}$ and $\mathcal{D}$ could be different. Besides, if $\mathcal{P}(\Delta E)$ has tails decreasing faster then the exponential, the large deviations functions of $\mathcal{W}$ and $\mathcal{D}$ are the same.

This scenario gives then simple hints for the knowledge of the large deviation functions of two time-extensive quantities which differs only by a stationary term. It turns out that if this stationary term is distributed with exponential tails, its fluctuations may affect the large deviation functions of the time-extensive quantities. This is clearly already seen in eq. (36), which shows that in this case fluctuations of order t are possible. This clearly does not happen if the tails of the pdf of the stationary term decrease faster than any exponential. In this case fluctuations of order t vanish in the infinite time limit, and the two large deviation functions are equal. Moreover, this scenario is perfectly in line with the explicit results obtained by Farago in several simple models [16, 26], and by Van Zon and Cohen in [27]. In all those solvable cases the system considered is a one-particle system, with a very low number of degrees of freedom. Hence, if the velocity of the particle has a Gaussian distribution, the energy pdf has exponential tails, and in principle the distribution of $\mathcal{W}$ and $\mathcal{D}$ can be different. Nevertheless, if the system under investigation is a many particle system, as it is the case here, the energy pdf is distributed following the gamma distribution [28]:

$$P(E) \sim E^{\frac{N}{2}-1} \exp(-E) \tag{38}$$

where N is the number of degrees of freedom of the system. Moreover, in the thermodynamic limit (i.e. when $N \to \infty$) the above expression of $P(E)$ approaches the Gaussian distribution. Thus, taking the thermodynamic limit before that of large times, it follows from the above discussion that for large systems (i.e. in the thermodynamic limit) the total work $\mathcal{W}$ and the dissipated energy $\mathcal{D}$ have the same large deviation function. This is in line with the observations of the previous subsection, which qualitatively predict the absence of a negative tail for $P(\mathcal{W})$.

F. The cumulants

In this section we find an approximated expression of $\mu(\lambda)$ solving a system of equations obtained projecting (27) on the first velocity moments. First we shall define a dimensionless velocity $\mathbf{c} = \mathbf{v}/v_0(\lambda)$, where $v_0(\lambda)$ plays the role of a thermal velocity:

$$v_0^2(\lambda) = 2T(\lambda) = \frac{2}{d} \int \mathrm{d}\mathbf{v}\, v^2\, \tilde{f}(\mathbf{v}, \lambda)\,. \tag{39}$$

Then, defining the function $f(\mathbf{c}, \lambda) = v_0(\lambda)^d \tilde{f}(\mathbf{v}, \lambda)$, and its related moments of order n

$$m_n(\lambda) = \int \mathrm{d}\mathbf{c}\, c^n f(\mathbf{c}, \lambda) \ , \tag{40}$$

one obtains the following recursion relation:

$$(\mu + \Gamma(2n+d)\lambda)m_n = \frac{\Gamma}{v_0^2} n(n+d-2)m_{n-2} + \Gamma\lambda^2 v_0^2 m_{n+2} - v_0\nu_n, \tag{41}$$

where

$$\nu_n = -\int \mathrm{d}\mathbf{c}\, c^n\, J[f,f]\ . \tag{42}$$

Recalling the definition of the cumulants (16), and the approximated solution for the stationary velocity pdf, it appears natural to argue that, for $\lambda \sim 0$, the function $f(\mathbf{c},\lambda)$ should be well approximated by an expansion around the Gaussian, in Sonine polynomials:

$$f(\mathbf{c},\lambda) = \phi(c)\left(1 + a_1(\lambda)S_1\left(c^2\right) + a_2(\lambda)S_2\left(c^2\right)\right) + \mathcal{O}(a_3)\ , \tag{43}$$

where $\phi(c) = \pi^{-d/2}\exp(-c^2)$ is the Gaussian distribution. Even in this case, from the relation (9) and from the definition (39), the coefficient a_1 is found to be 0. The method consists in taking the equation (41) for $n = 0$, 2 and 4 in order to find an explicit expression of μ, v_0, and a_2 in the limit $\lambda \to 0$. The quantities ν_2 and ν_4 have been calculated at the first order in a_2 [22], and their explicit expressions are:

$$\nu_2 = \frac{(1-\alpha^2)}{2\ell}\frac{\Omega_d}{\sqrt{2\pi}}\left\{1 + \frac{3}{16}a_2\right\} = \frac{d\Gamma}{\sqrt{2T_0^3}}\left\{1 + \frac{3}{16}a_2\right\}\ , \tag{44}$$

and

$$\nu_4 = \frac{d\Gamma}{\sqrt{2T_0^3}}\left\{T_1 + a_2 T_2\right\}, \tag{45}$$

with

$$T_1 = d + \frac{3}{2} + \alpha^2 \tag{46}$$

$$T_2 = \frac{3}{32}(10\,d + 39 + 10\,\alpha^2) + \frac{(d-1)}{(1-\alpha)}, \tag{47}$$

where $T_0 = \left(\frac{2d\Gamma\ell\sqrt{\pi}}{(1-\alpha^2)\Omega_d}\right)^{2/3}$ is the the granular temperature obtained averaging over Gaussian velocity pdfs (i.e. the zero-th order of Sonine expansion). The expression of the first moments m_n is:

$$m_0 = 1 \tag{48a}$$

$$m_2 = d/2 \tag{48b}$$

$$m_4 = \frac{(1+a_2)\ d\ (2+d)}{4} \tag{48c}$$

$$m_6 = \frac{(1+3\,a_2)\ d\ (2+d)\ (4+d)}{8} \tag{48d}$$

With the help of the above defined temperature scale T_0, we shall now introduce some dimensionless variables:

$$\begin{aligned} \tilde{\mu} &= \mu\frac{T_0}{d\Gamma}, & \tilde{\lambda} &= \lambda T_0, \\ \tilde{v}_0^2 &= \frac{v_0^2}{2T_0}, & \tilde{\nu}_p &= \frac{\sqrt{2\,T_0^3}}{\Gamma}\nu_p\,. \end{aligned} \tag{49}$$

Note that this scaling naturally defines the scales for the other quantities of interest, namely:

$$\tilde{\pi}_t = \pi_t\frac{T_0}{d\Gamma}, \qquad \tilde{w} = \frac{w}{d\Gamma}, \qquad \tilde{\mathcal{W}} = \frac{\mathcal{W}}{\langle\mathcal{W}\rangle}\ . \tag{50}$$

The expression of the moment equation (41) becomes, for the above defined dimensionless quantities:

$$\left(\tilde{\mu}d + (2n+d)\tilde{\lambda}\right)m_n = \frac{n(n+d-2)}{2\tilde{v}_0^2}m_{n-2} + 2\tilde{\lambda}^2\tilde{v}_0^2 m_{n+2} - \tilde{v}_0\tilde{\nu}_n\ . \tag{51}$$

First we solve the above equation for $n = 0$, getting the following result:

$$\tilde{\mu}(\tilde{\lambda}) = -\tilde{\lambda} + \tilde{\lambda}^2 \tilde{v}_0^2(\tilde{\lambda}). \tag{52}$$

Recalling that when $\lambda \to 0$ one has $v_0^2 = 2T_g + \mathcal{O}(\lambda)$, it is important to note that if we restrict our analysis to the Gaussian approximation for $P(\mathcal{W}, t)$, that is if we truncate $\mu(\lambda)$ to order λ^2, Eq. (52) will read:

$$\frac{\mu}{d\Gamma} = \lambda(\lambda T_g - 1) \ . \tag{53}$$

Then we see that indeed

$$\mu(\lambda) = \mu \left(\frac{1}{T_g} - \lambda \right) \ , \tag{54}$$

which means that $\pi_\infty(w) = \max_\lambda\{\mu(\lambda) + \lambda w\}$ verifies

$$\pi_\infty(w) - \pi_\infty(-w) = \frac{w}{T_g} \ . \tag{55}$$

This is, up to a prefactor T_g, the GCFR. However, the nontrivial functions $m_n(\lambda)$ will break the property (54), as we shall explicitly show later. In order to characterize more precisely the dependence of $\tilde{\mu}$ upon $\tilde{\lambda}$ for small values of $\tilde{\lambda}$, it is useful to expand $\tilde{v}_0^2$ and a_2 in powers of $\tilde{\lambda}$:

$$\tilde{v}_0^2(\tilde{\lambda}) = \tilde{v}_0^{2^{(0)}} + \tilde{\lambda}\tilde{v}_0^{2^{(1)}} + \tilde{\lambda}^2 \tilde{v}_0^{2^{(2)}} + \mathcal{O}(\tilde{\lambda}^3) \tag{56a}$$

$$a_2(\tilde{\lambda}) = a_2^{(0)} + \tilde{\lambda} a_2^{(1)} + \tilde{\lambda}^2 a_2^{(2)} + \mathcal{O}(\tilde{\lambda}^3) \tag{56b}$$

In this way we can find $\tilde{v}_0^{2^{(i)}} \left(a_2^{(i)} \right)$ solving equation (51) for $n = 2$:

$$\tilde{v}_0^{2^{(0)}} = \left(1 - \frac{a_2^{(0)}}{8} \right) \ , \tag{57}$$

$$\tilde{v}_0^{2^{(1)}} = -\frac{4}{3} + \frac{a_2^{(0)}}{3} - \frac{a_2^{(1)}}{8} \ , \tag{58}$$

$$\tilde{v}_0^{2^{(2)}} = 2 - a_2^{(0)} \left(\frac{1}{12} + \frac{d}{3} \right) + \frac{a_2^{(1)}}{3} - \frac{a_2^{(2)}}{8} \ . \tag{59}$$

Then we substitute $\tilde{v}_0^2(\tilde{\lambda})$ in the third equation and expand it in powers of $\tilde{\lambda}$ to find the expression of $a_2^{(i)}(\alpha)$. Note that one has also to expand in powers of a_2 and keep only the linear terms in order to be coherent with the $\tilde{\nu}_p$-s calculations. We find the following expressions, which are plotted in Fig. 1:

$$a_2^{(0)} = \frac{4 \ (1-\alpha) \ \left(1 - 2\,\alpha^2\right)}{19 + 14\,d - 3\,\alpha\,(9 + 2d) + 6(1-\alpha)\,\alpha^2} \tag{60}$$

$$a_2^{(1)} = -\frac{4\,(1-\alpha)^2 \ \left(-1 + 2\,\alpha^2\right) \ \left(31 + 2\,\alpha^2 + 16\,d\right)}{(19 + 14\,d - 3\,\alpha\,(9 + 2d) + 6(1-\alpha)\,\alpha^2)^2} \tag{61}$$

$$a_2^{(2)} = \frac{A(\alpha)}{B(\alpha)} \tag{62}$$

with

$$\begin{aligned} A(\alpha) = 16\,(-1+\alpha)^2 \ \left(-1 + 2\,\alpha^2\right) \ \{906 + \alpha \ [-984 + \alpha \ (85 + 3\,\alpha \ (-19 + 6 \ (-1+\alpha) \ \alpha))] + 985\,d + \\ + \alpha \ [-951 + \alpha \ (-25 + 3\,\alpha \ (7 + 6 \ (-1+\alpha) \ \alpha))] \ d + (269 + 3\,\alpha \ (-75 + 2\,\alpha \ (-7 + 3\,\alpha))) \ d^2\} \, , \end{aligned} \tag{63}$$

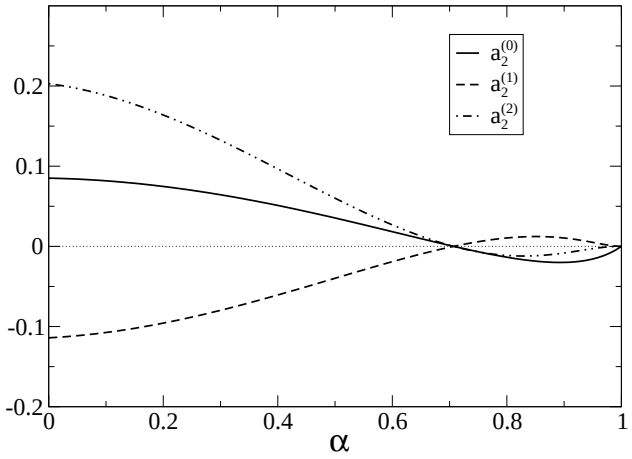

FIG. 1: $a_2^{(0)}$, $a_2^{(1)}$ and $a_2^{(2)}$ versus α for inelastic hard spheres driven by random forces in $d = 2$.

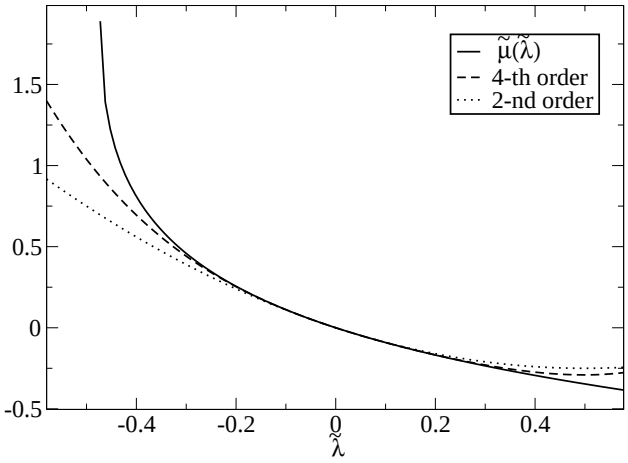

FIG. 2: The solid line shows $\tilde{\mu}$ in the limit $d \to \infty$ for inelastic hard spheres. The dashed line is $\tilde{\mu}$ at fourth order in $\tilde{\lambda}$ from (52) for $d = 2$ and $\alpha = 0.5$. Finally the dotted line shows the same quantity calculated with a truncation at second order in λ, which would satisfy the GCFR.

and

$$B(\alpha) = 3\left(-19 - 14\,d + 3\,\alpha\,\left(9 + 2\,\left(-1 + \alpha\right)\,\alpha + 2\,d\right)\right)^3 \tag{64}$$

The $v_0^{2^{(0)}}$ expression, as well as the $a_2^{(0)}$ expression, coincide with the usual results established for granular gases [22, 23]. At this point the computation of the cumulants becomes straightforward. From relation (16) it follows:

$$\lim_{t\to\infty} \frac{\langle \mathcal{W}^n \rangle_c}{t} = (-1)^n d\Gamma T_0^{n-1} n!\ \tilde{v}_0^{2^{(n-2)}}\ . \tag{65}$$

Moreover, since the $a_2^{(i)}$ corrections are numerically small, as shown in Fig. 1, the zero-th order (Gaussian) approximation already gives a good estimate for the cumulants. Namely, the first cumulants are , in this approximation:

$$\begin{aligned} \langle \mathcal{W} \rangle_c &= tNd\Gamma\ , & \left\langle \mathcal{W}^2 \right\rangle_c &= 2tNd\Gamma T_0\ , \\ \left\langle \mathcal{W}^3 \right\rangle_c &= 8tNd\Gamma T_0^2\ , & \left\langle \mathcal{W}^4 \right\rangle_c &= 48tNd\Gamma T_0^3\ . \end{aligned} \tag{66}$$

All the above expansions in powers of λ, at the second order in Sonine coefficients (e.g. a_2) can be carried out by expanding v_0 and a_2 in (56) to higher powers of λ. Moreover, expanding in higher order in Sonine coefficient (e.g. a_3) remains in principle still possible, but will involve a higher number of equations in the hierarchy (51) (e.g. $n = 6$), and therefore will need the expression of higher order collisional moments (e.g. ν_6).

G. The solvable infinite dimension limit

The previous discussion strongly suggests that at high dimensions $\tilde{f}(\mathbf{v}, \lambda)$ is not far from a Gaussian. First, the inspection of the $d \to \infty$ limit of the Sonine expansion performed in the previous subsection indicates that the corrections to the Gaussian (see formula 60 and 61) carry a relative d^{-1} factor, thus leaving the Gaussian pdf as the leading behavior when $d \to \infty$. Second, the $\lambda = 0$ case is well known to reproduce a Gaussian in the $d \to \infty$ limit: there is numerical evidence that the collision integral is solved (i.e. is set to zero) by a Gaussian $\tilde{f}$, when $d \to \infty$. Of course if the Gaussian solves the collision integral then it solves the whole equation.

We are therefore led to consider, in the limit $d \to \infty$, $\tilde{f}(\mathbf{v}, \lambda)$ to be a Gaussian with a λ-dependent second moment. In this situation the dimensionless function f will read:

$$f(\mathbf{c}) = \frac{e^{-c^2}}{\pi^{d/2}} \tag{67}$$

with $\mathbf{c}(\lambda) = \mathbf{v}/v_0(\lambda)$. In this context one can solve equation (51) in order to get an explicit expression for $\mu(\lambda)$. The equation defined by (51) for $n = 0$ gives:

$$\tilde{\mu}(\tilde{\lambda}) = -\tilde{\lambda} + \tilde{\lambda}^2 \tilde{v}_0^2(\tilde{\lambda}) \,, \tag{68}$$

where $\tilde{v}_0^2(\tilde{\lambda})$ is obtained from Eq. (51) for $n = 2$, which reads:

$$\tilde{\lambda}^2 \tilde{v}_0^4 - \tilde{v}_0^3 - 2\tilde{\lambda}\tilde{v}_0^2 + 1 = 0 \quad . \tag{69}$$

The unique solution of the above equation which verifies the physical requirement $\tilde{v}_0^2(0) = 1$ is:

$$\tilde{v}_0^2(\tilde{\lambda}) = \frac{1 + 4\,\tilde{\lambda}^3}{4\,\tilde{\lambda}^4} + \frac{b_1(\tilde{\lambda})}{2} - \frac{1}{2}\left[-\frac{8}{\tilde{\lambda}^2} + \frac{\left(1 + 4\,\tilde{\lambda}^3\right)^2}{2\,\tilde{\lambda}^8} + b_2(\tilde{\lambda}) - b_3(\tilde{\lambda}) + \frac{b_4(\tilde{\lambda})}{4 b_1(\tilde{\lambda})} \right]^{\frac{1}{2}} \quad , \tag{70}$$

with

$$\begin{aligned} b_1(\tilde{\lambda}) &= \sqrt{\frac{\tilde{\lambda}^{-8}}{4} + \frac{2}{\tilde{\lambda}^5} - b_2(\tilde{\lambda}) + b_3(\tilde{\lambda})} \,, \quad b_2(\tilde{\lambda}) = \frac{4\left(\frac{2}{3}\right)^{\frac{1}{3}}}{\tilde{\lambda}^3 \left(9 + \sqrt{3}\,\sqrt{27 + 256\,\tilde{\lambda}^3}\right)^{\frac{1}{3}}} \,, \\ b_3(\tilde{\lambda}) &= \frac{\left(9 + \sqrt{3}\,\sqrt{27 + 256\,\tilde{\lambda}^3}\right)^{\frac{1}{3}}}{2^{\frac{1}{3}}\, 3^{\frac{2}{3}}\, \tilde{\lambda}^4} \,, \quad b_4(\tilde{\lambda}) = \frac{32}{\tilde{\lambda}^3} - \frac{24\,\left(1 + 4\,\tilde{\lambda}^3\right)}{\tilde{\lambda}^6} + \frac{\left(1 + 4\,\tilde{\lambda}^3\right)^3}{\tilde{\lambda}^{12}} \,. \end{aligned} \tag{71}$$

This expression of the velocity scale reduces to the kinetic temperature for $\lambda = 0$, and decreases monotonically as $\lambda^{-1/2}$ when $\lambda \to \infty$. This means that in the limit $\lambda \to \infty$ $\tilde{f}$ approaches a Dirac distribution as $\exp(-\lambda v^2/2)$. This feature supports the intuition that the small $\mathcal{W}$ events (which are related to the large values of λ) are provided by the small velocities. The behavior of $\tilde{\mu}$ is shown in Fig. 2. The large deviations function $\tilde{\mu}(\tilde{\lambda})$ becomes complex for $\tilde{\lambda} < -\frac{3}{2^{8/3}}$, because of the terms containing $\sqrt{27 + 256\tilde{\lambda}^3}$. Moreover for large $\tilde{\lambda}$ the behavior of this function is $\tilde{\mu}(\tilde{\lambda}) \sim -\tilde{\lambda}^{\frac{1}{4}}$. In the vicinity of the singularity (i.e. $\tilde{\lambda} = \lambda_0 = -\frac{3}{2^{8/3}}$) the behavior of the large deviation function is:

$$\tilde{\mu}(\tilde{\lambda}) = \frac{3}{2^{2/3}} - 3^{3/2} 2^{1/6} \sqrt{\tilde{\lambda} - \lambda_0} + \mathcal{O}(\tilde{\lambda} - \lambda_0) \,. \tag{72}$$

From the behavior for large $\tilde{\lambda}$ it is possible to recover the left tail of the large deviation function π_∞. In general, if $\mu(\lambda) \sim -\lambda^\beta$ for $\lambda \to \infty$, this leads to $\mu'(\lambda_*) = -\beta\lambda_*^{\beta-1} = -w$. This last relation tells us that for $\beta < 1$ we are recovering the limit $w \to 0^+$, with a behavior of the large deviation function given by $\pi_\infty(w) = \mu(\lambda_*) + \lambda_* w \sim w^{\frac{\beta}{\beta-1}}$. Moreover, from the behavior of μ near λ_0, an analogous calculation provides the right tail of the large deviation function: $\pi_\infty(w) \sim \lambda_0 w$, when $w \to \infty$. Finally, in our particular case, the tails are given by

$$\tilde{\pi}_\infty(\tilde{w} \to 0^+) \sim -\tilde{w}^{-1/3} \;,\; \tilde{\pi}_\infty(\tilde{w} \to \infty) \sim -\tilde{w} \;, \tag{73}$$

Note that, as expected from the discussion in subsection II E, there is no $w < 0$ tail to $\tilde{\pi}_\infty$. The graph of the whole function $\tilde{\pi}_\infty(\tilde{w})$ is depicted in Fig. 3.

III. INELASTIC MAXWELL GAS

A. The model

The Maxwell gas is a kinetic model due to J.C. Maxwell, who observed that a pair potential proportional to $r^{-2(d-1)}$, being r the distance between two interacting particles, gives rise to a great simplification of the collision integral [29]. In fact this kind of interaction makes the collision frequency velocity independent. It must be noted that when the inelasticity of the particles is considered, this model looses its well-defined physical interpretation, but it nevertheless keeps its own interest. The collision integral is analytically simpler than the hard particles model and preserves the essential physical ingredients in order to have qualitatively the same phenomenology. In the recent development of granular gases this kinetic model has been extensively investigated [30, 31, 32, 33]. In particular Inelastic Maxwell

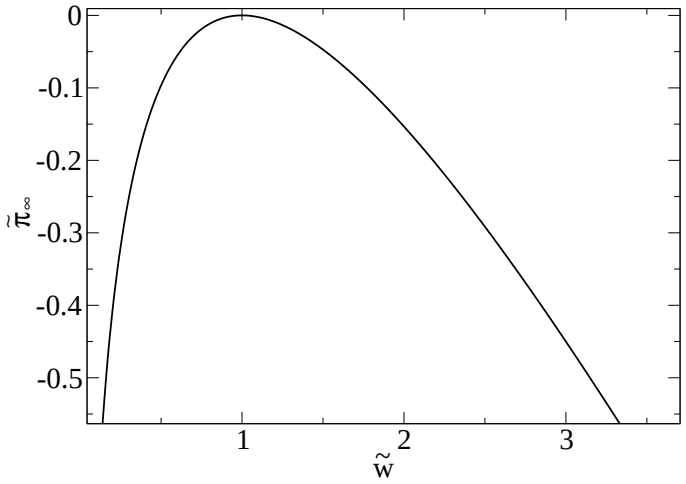

FIG. 3: Large deviation function $\tilde{\pi}_\infty(\tilde{w})$ for $d = \infty$, as obtained by numerical inverse Legendre transform of Eq. (68).

molecules display strong non-Gaussian velocity pdfs (generally stronger than for the hard spheres), which can be even pathological in some cases. For example the velocity pdf of the cooling regime of such a gas has tails with algebraic decay. Nevertheless for the stochastically driven gas such a pathology does not exists, and the tails of the velocity pdf have an exponential decay. Moreover, as it will appear in the next section, with this model the DSMC simulation algorithm is highly optimized, and thus a much more precise observation of rare events can be achieved.

The Boltzmann equation governing the single particle velocity distribution is:

$$\partial_t f(\mathbf{v}_1, t) = J_M[f, f] + \Gamma \Delta_{\mathbf{v}_1} f(\mathbf{v}_1) \ , \tag{74}$$

where J_M is the collision integral, which slightly changes from (6):

$$J_M[f, f] = \omega_0 \int \mathrm{d}\mathbf{v}_2 \int \mathrm{d}\hat{\boldsymbol{\sigma}} \left(\frac{f(\mathbf{v}_1^{**}) f(\mathbf{v}_2^{**})}{\alpha} - f(\mathbf{v}_1) f(\mathbf{v}_2) \right) . \tag{75}$$

The solution of such equation have been extensively analyzed [30, 31, 32], and it turns out that even in this case a Sonine expansion up to the second order provides a good estimate of the pdf for low velocities, while the tails of the pdf are exponential.

In order to compute the large deviation function associated to the total work distribution, the same reasoning carried out in the previous part still holds. Thus, the analogous of equation (27) becomes, for Maxwell molecules:

$$\begin{aligned} \mu \tilde{f}(\mathbf{v}, \lambda, t) =& \Gamma \Delta_{\mathbf{v}} \tilde{f} + 2\lambda \Gamma \mathbf{v} \cdot \partial_{\mathbf{v}} \tilde{f} + \Gamma(d\lambda + \lambda^2 v^2) \tilde{f} \\ &+ \omega_0 \int \mathrm{d}\mathbf{v}_2 \int \mathrm{d}\hat{\boldsymbol{\sigma}} \left[\alpha^{-1} \tilde{f}(\mathbf{v}_1^{**}, \lambda) \tilde{f}(\mathbf{v}_2^{**}, \lambda) - \tilde{f}(\mathbf{v}_1, \lambda) \tilde{f}(\mathbf{v}_2, \lambda) \right] \ , \end{aligned} \tag{76}$$

where the same molecular-chaos-like assumption as in section II has been implemented.

B. The cumulants

In this section we will provide the computation of the cumulants for the integrated power injected by the thermostat. The procedure is formally the same as in the previous section, for the hard sphere gas. The recursive equation involving the velocity moments is found from (76), and reads:

$$(\mu + \Gamma(2n + d)\lambda) m_n = \frac{\Gamma}{v_0^2} n(n + d - 2) m_{n-2} + \Gamma \lambda^2 v_0^2 m_{n+2} - \omega_0 \nu_n \ , \tag{77}$$

where m_n is the $n-$th moment related to the dimensionless function f (cf. eq (40)). The expression of the collisional moments is now slightly different. The two first non-vanishing moments are [34]:

$$\nu_2 = \frac{1 - \alpha^2}{4} = \frac{d\Gamma}{\omega_0 T_0} \ , \tag{78}$$

and

$$\nu_4 = \frac{\nu_2}{8}(T_1 + a_2 T_2) \ , \tag{79}$$

with

$$T_1 = 2(5 + 3\alpha^2 + 4d) \ , \tag{80}$$

$$T_2 = 3\alpha^2 - \frac{\alpha(17+4d) - 3(3+4d)}{1-\alpha} \ . \tag{81}$$

Here again $T_0 = \frac{4d\Gamma}{\omega_0(1-\alpha^2)}$ denotes the zero-th order temperature. Let us introduce the following rescaled variables:

$$\begin{aligned} \tilde{\mu} &= \mu \frac{T_0}{d\Gamma} & \tilde{\lambda} &= \lambda T_0 \\ \tilde{v}_0^2 &= \frac{v_0^2}{2T_0} & \tilde{\nu}_p &= \frac{\omega_0 \, T_0}{d\Gamma} \nu_p \end{aligned} \tag{82}$$

The equation for the moment reads for the dimensionless variables:

$$(d\tilde{\mu} + (2n+d)\tilde{\lambda}) m_n = \frac{1}{2\tilde{v}_0^2} n(n+d-2) m_{n-2} + 2\tilde{\lambda}^2 \tilde{v}_0^2 m_{n+2} - d\tilde{\nu}_n \ . \tag{83}$$

Expanding again the solution in a Gaussian distribution multiplied by a series of Sonine polynomials up to the second order one obtains, from the first three equations of the hierarchy (83), a closed set of equations involving $\tilde{\mu}$, $\tilde{v}_0^2$ and a_2. Those equations can be solved in the vicinity of $\lambda = 0$ and in the limit of small non-Gaussianity ($|a_2(\lambda)| \ll 1$), when linearized with respect to the coefficient a_2. In this framework, which should be valid in the limit of small values of $\tilde{\lambda}$, the solution is:

$$\mu(\lambda) = \frac{1 - \sqrt{1+4\,\lambda}}{2} - a_2 \, \frac{(2+d)\, \left(-1 + \sqrt{1+4\,\lambda} + 2\,\lambda\, \left(-2 - \lambda + \sqrt{1+4\,\lambda}\right)\right)}{4\,\sqrt{1+4\,\lambda}} + \mathcal{O}(a_2^2) \tag{84}$$

with

$$a_2(\lambda) = \frac{-6\,(1-\alpha)^2\,(1+\alpha)}{(1+\alpha)\,(7+3\,(\alpha-2)\,\alpha - 4\,d) + 8\,(\alpha-1)\,(2+d)\,\sqrt{1+4\,\lambda}} \ . \tag{85}$$

Expanding this expression in powers of $\tilde{\lambda}$, it is possible to recover all the coefficients $a_2^{(i)}$ of the expansion (56). The first coefficients are plotted in Fig. 4. These results allows us to directly compute the cumulants from the derivatives of $\tilde{\mu}$:

$$\langle \mathcal{W}^n \rangle_c = d\Gamma T_0^{n-1} \left. \frac{\mathrm{d}^n \tilde{\mu}}{\mathrm{d}\tilde{\lambda}^n} \right|_{\tilde{\lambda}=0} \ . \tag{86}$$

It turns out that the corrections coming from the Sonine expansion are small with respect to the Gaussian order, which therefore already provides a good estimate. The values of the first cumulants are:

$$\begin{aligned} \langle \mathcal{W} \rangle_c &= tNd\Gamma \ , & \left\langle \mathcal{W}^2 \right\rangle_c &= 2tNd\Gamma T_0 \ , \\ \left\langle \mathcal{W}^3 \right\rangle_c &= 12tNd\Gamma T_0^2 \ , & \left\langle \mathcal{W}^4 \right\rangle_c &= 120tNd\Gamma T_0^3 \ . \end{aligned} \tag{87}$$

C. The solvable infinite dimension limit

In this section we will provide an exact solution for the generating function $\mu(\lambda)$ in the infinite dimension limit. As already noted by Ben-Naim and Krapivsky, in this limit the velocity pdf approaches the Gaussian distribution [31]. Therefore, we will show that a Maxwellian with a variance depending on λ is indeed a solution of equation (76).

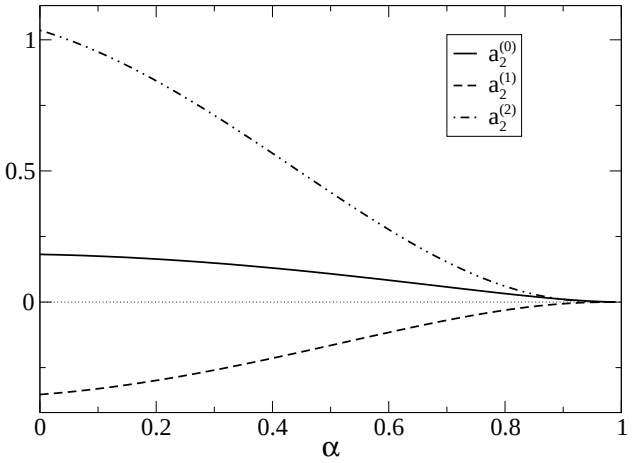

FIG. 4: $a_2^{(0)}$, $a_2^{(1)}$ and $a_2^{(2)}$ versus α for the inelastic Maxwell model in $d = 2$.

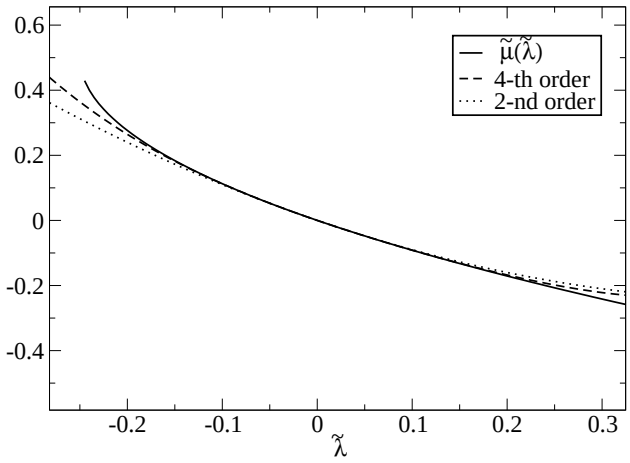

FIG. 5: The solid line shows $\tilde{\mu}$ in the limit $d \to \infty$ for the inelastic Maxwell model, given in Eq. (96). The dashed line is $\tilde{\mu}$ at fourth order in $\tilde{\lambda}$ from (84) for $d = 2$ and $\alpha = 0.5$. Finally the dotted line shows the same quantity calculated with a truncation at second order in λ, which would satisfy the GCFR.

Because of the convolution structure of the collision integral, a great simplification occurs introducing the Fourier Transform of the velocity pdf:

$$F(\mathbf{k}, \lambda) = \int \mathrm{d}\mathbf{v}\, \mathrm{e}^{i\mathbf{k}\cdot\mathbf{v}} f(\mathbf{v}, \lambda)\,. \tag{88}$$

Assuming that F is an isotropic function of the wave vector $\mathbf{k}$, the equation (76) reads:

$$\mu F(k) = -\Gamma k^2 F(k) - \lambda\Gamma d F(k) - 2\lambda\Gamma k \frac{\partial F(k)}{\partial k} - \lambda^2\Gamma \frac{\partial^2 F(k)}{\partial k^2} + \omega_0 \left\langle F(\sqrt{\xi}k) F(\sqrt{\eta}k) \right\rangle_\theta - \omega_0 F(k) \tag{89}$$

where

$$\xi = 1 - \left(1 - \left(\frac{1-\alpha}{2}\right)^2\right)\theta \quad , \quad \eta = \left(\frac{1+\alpha}{2}\right)^2 \theta\,, \tag{90}$$

and the brackets with a subscript θ denote an angular average

$$\langle f \rangle_\theta = \int_0^1 d\theta \frac{\theta^{-\frac{1}{2}} (1-\theta)^{\frac{d-3}{2}}}{B\left(\frac{1}{2}, \frac{d-1}{2}\right)} f(\theta)\,, \tag{91}$$

where B is the beta function. Injecting a Gaussian solution $\phi(k) = \mathrm{e}^{-\frac{k^2 T}{2}}$ into the above equation yields the following relation:

$$\mu = -\Gamma k^2 - \lambda d\Gamma + 2\lambda k^2 T + \lambda^2 \Gamma T - \lambda^2 \Gamma k^2 T^2 + \omega_0 \left\langle \mathrm{e}^{-\frac{k^2(1-\alpha^2)\theta T}{4}} \right\rangle_\theta - \omega_0\,. \tag{92}$$

Then, expanding the exponential term in a power series and using that

$$\langle \theta^p \rangle_\theta = \frac{\Gamma(\frac{d}{2})\Gamma(p+\frac{1}{2})}{\Gamma(\frac{1}{2})\Gamma(p+\frac{d}{2})} \sim \frac{1}{d^p}\,, \tag{93}$$

when $d \to \infty$, one sees that the above relation holds for each k, with:

$$\mu(\lambda) = -\lambda d\Gamma + \lambda^2 \Gamma T(\lambda) \tag{94}$$

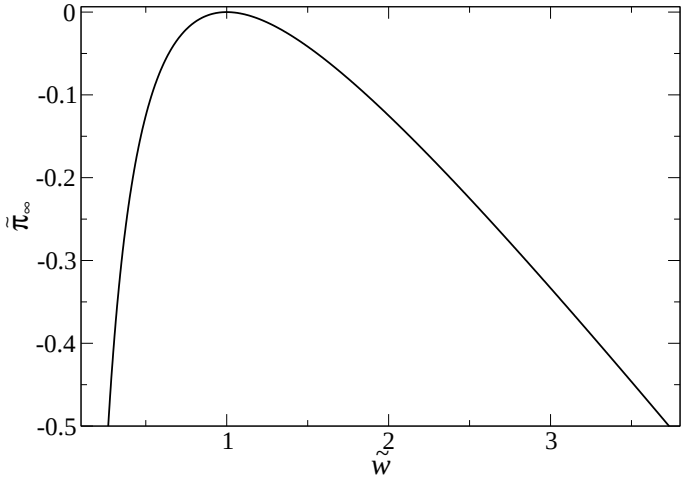

FIG. 6: $\tilde{\pi}_\infty(\tilde{w})$ for the Inelastic Maxwell Model in the limit $d \to \infty$.

and,

$$T(\lambda) = \frac{1 + 2\,\lambda\,T_0 - \sqrt{1 + 4\,\lambda\,T_0}}{2\,\lambda^2\,T_0} \tag{95}$$

where T_0 is the granular temperature. Hence, the explicit form of the generating function is, using the rescaled variables defined in (82) is:

$$\tilde{\mu}(\tilde{\lambda}) = \frac{1 - \sqrt{1 + 4\,\tilde{\lambda}}}{2}\ . \tag{96}$$

This function has the same behavior as its analogous for the IHS gas, since it presents a cut in the negative real axis (for $\lambda < -1/4$), and it decreases monotonically (as $-\lambda^{1/2}$) when $\lambda \to \infty$. Furthermore this expression is, up to irrelevant constants, exactly the same as the one found in a simpler system, the Ornstein-Ulhenbeck process, which has been extensively analyzed by Farago in [16, 26]. The analytical expression of the large deviation function for the total work is easily computed as the Legendre transform of the above expression of $\tilde{\mu}(\tilde{\lambda})$. It reads:

$$\tilde{\pi}_\infty(\tilde{w}) = -\frac{(\tilde{w} - 1)^2}{4\tilde{w}}\,\Theta(\tilde{w})\ . \tag{97}$$

This function is plotted in Fig. 6. One can easily see that even for this model there are no negative events in the large time limit. The left tail of the large deviation function decrease to $-\infty$ as $-1/4\tilde{w}$, while the right tail has a linear decreasing behavior.

IV. NUMERICAL RESULTS

In this section the results of numerical simulations of the two models (inelastic hard spheres and inelastic Maxwell model) are presented with particular attention to the Fluctuation Relation for the injected power. We emphasize that obviously only $\pi_t(w)$ can be accessed numerically whereas the GCFR bears on $\pi_\infty(w)$. This requires a precise discussion of finite time effects, that play a crucial role here. The main requirement to verify the validity of the Fluctuation Relation is a clean observation of a negative tail in the pdf of the injected power. This poses a dramatic limit to the time t of integration of $\mathcal{W}(t)$. In numerical simulations, as well as in real experiments, at times larger than a few mean free times the negative tail disappears. On the other hand, at times of the order of 1-3 mean free times, the Fluctuation Relation appears to be correctly verified for the inelastic Hard Spheres model and slightly violated for the inelastic Maxwell model. The measure of the cumulants, anyway, gives a neat indication of the fact that the time of convergence of the large deviation function is at least 10 times larger and that the true asymptotic is well reproduced by the theory exposed in this article.

The stationary state of a driven granular gas, modeled by equation (5), under the assumption of Molecular Chaos, is very well reproduced by a Direct Simulation Monte Carlo [23, 25]. As a first check of reliability of the algorithm,

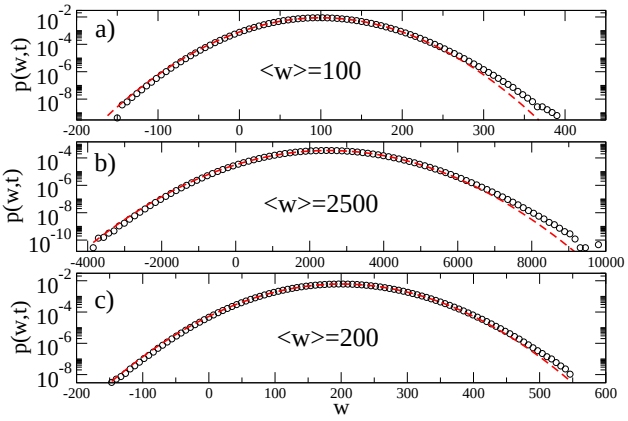

FIG. 7: Probability density function of the injected power, $p(w,t) \equiv tP(\mathcal{W}(t) = wt, t)$ with t equal to 1 mean free time. In all three cases the value of the restitution coefficient is $\alpha = 0.9$. Other parameters are a) $N = 100$, $\Gamma = 0.5$; b) N=100, $\Gamma = 12.5$; c) $N = 200$, $\Gamma = 0.5$. The dashed line represents a Gaussian with the same first two cumulants. These distributions have been obtained with $\sim 1.5 \times 10^9$ independent values of $\mathcal{W}(t)$.

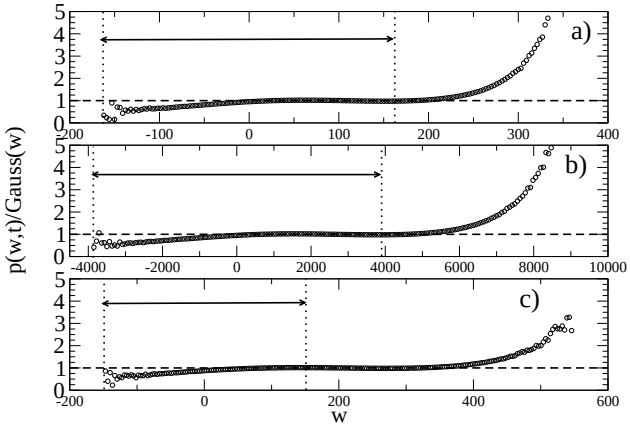

FIG. 8: Ratio of $P(\mathcal{W}, t)$ and a Gaussian with the same first two moments, for the same parameters as in figure 7: a) corresponds to $N = 100$, $\Gamma = 0.5$, b) to $N = 100$, $\Gamma = 12.5$ and c) to $N = 200$, $\Gamma = 0.5$. The range between the vertical dotted lines is the useful one for the check of the Gallavotti-Cohen relation. It can be noted that the strongest deviations from the Gaussian behavior appear outside of this range.

we have measured the granular temperature T_g and the first non-zero Sonine coefficient $a_2 \equiv (\langle v^4 \rangle / \langle v^2 \rangle^2 - 3)/3$. The measured granular temperature is always in perfect agreement with the estimate. The measured a_2 coefficient is a highly fluctuating quantity and its average is in very good agreement with the theoretical estimate.

A. Inelastic Hard spheres

In Fig. 7, the probability density functions $p(w,t) \equiv tP(wt,t)$ (only for t equal to 1 mean free time) for three different choices of parameters N, Γ (at fixed restitution coefficient α) is shown. The values of the first two cumulants of the distribution and their theoretical values are compared in table I, with very good agreement. In the same table we present also the measure of the third and fourth rescaled cumulants. The formulae for the first few cumulants are:

$$\langle x \rangle_c = \langle x \rangle \tag{98a}$$
$$\langle x^2 \rangle_c = \langle x^2 \rangle - \langle x \rangle^2 \tag{98b}$$
$$\langle x^3 \rangle_c = \langle x^3 \rangle - 3\langle x^2 \rangle \langle x \rangle + 2\langle x \rangle^3 \tag{98c}$$
$$\langle x^4 \rangle_c = \langle x^4 \rangle - 4\langle x^3 \rangle \langle x \rangle + 12\langle x^2 \rangle \langle x \rangle^2 - 6\langle x \rangle^4 - 3\langle x^2 \rangle^2 \tag{98d}$$
$$\tag{98e}$$

N	Γ	$\langle \mathcal{W}(t) \rangle / t$	$\langle \mathcal{W}(t)^2 \rangle_c / t$	$N\Gamma d$	$2N\Gamma d T_g$	$\sqrt{t}\ \sigma(t)$	$t\ \kappa(t)$
100	0.5	100	20835	100	21052	0.200432	0.355176
100	12.5	2500	13019125	2500	13157900	0.201739	0.361635
200	0.5	199.9	42009	200	42120	0.141589	0.175454

TABLE I: First cumulants, together with the skewness $\sigma(t) = \langle \mathcal{W}(t)^3 \rangle_c / \left(\langle \mathcal{W}(t)^2 \rangle_c \right)^{3/2}$ and the kurtosis excess $\kappa(t) = \langle \mathcal{W}(t)^4 \rangle_c / \left(\langle \mathcal{W}(t)^2 \rangle_c \right)^2$ of the distribution of injected work $P(\mathcal{W}, t)$, measured with t equal to 1 mean free time for different choices of the parameters.

The comparison with a Gaussian with same mean value and same variance shows that the pdf $P(\mathcal{W}, t)$ is not exactly a Gaussian. In particular there are deviations from the Gaussian form in the right (positive) tail. This is well seen in Fig. 8. It must be noted that the largest deviations in the right tail arise at values of $\mathcal{W}(t)$ larger than the minimum

$\mathcal{W}(t)$ available in the left tail, i.e. they have no influence in the following plot of Fig. 9 regarding the Gallavotti-Cohen symmetry.

In Fig. 9, the finite time Gallavotti-Cohen relation $\pi_t(w) - \pi_t(-w) = \beta_{eff} w$ is tested for the same choices of the parameters. The relation, at this level of resolution and for this value of the time t (1 mean free time), is well satisfied. Moreover table II shows that the value of β_{eff} is well approximated by $1/T_g$, as expected if the truncation of $\mu(\lambda)$ at the second order were valid, see eq. (55). In Fig. 10 the same relation is checked for different, slightly larger values of t (i.e. up to t equal to 3 mean free times). No relevant deviations are observed as t is increased. Moreover this figure is important to understand the dramatic consequences that larger t have on the possibility to check numerically the Gallavotti-Cohen symmetry: as t is increased, events with negative integrated power injection become rarer and rarer. This eventually leads to the vanishing of the left branch of $P(\mathcal{W}, t)$.

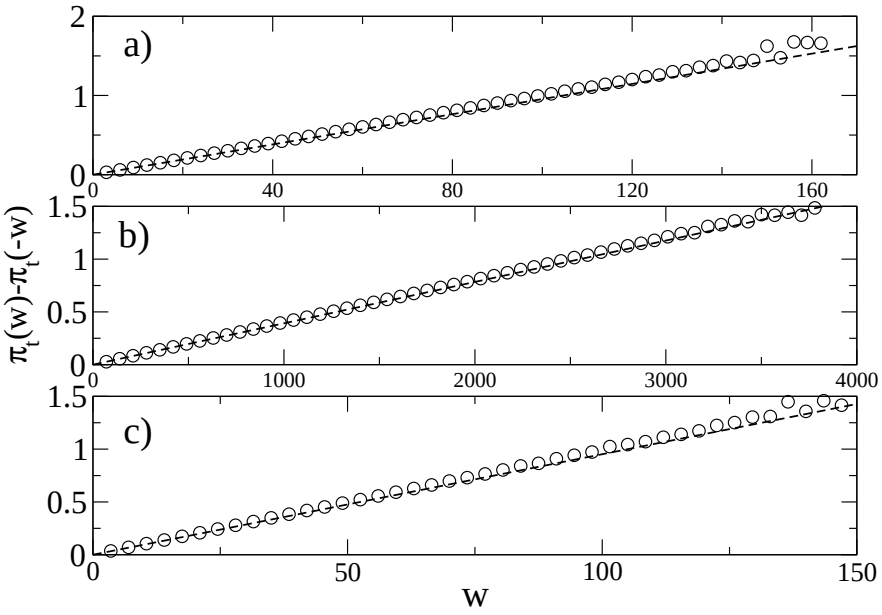

FIG. 9: Test of the Gallavotti-Cohen relation $\pi_t(w) - \pi_t(-w) = \beta_{eff} w$, for the same choices of the parameters as in Fig. 7. The values of the slope β_{eff} of the fitting dashed lines are in table II

.

N	Γ	β_{eff}	$1/T_g$
100	0.5	0.0100	0.00955
100	12.5	0.000402	0.000382
200	0.5	0.00995	0.00952

TABLE II: Factor of proportionality in the "Gallavotti-Cohen" relation compared with $\beta = 1/T_g$.

The main conclusion is that no appreciable departure from the λ^2 truncation is observed at this level of resolution. Much larger statistics are required to probe the very high energy tails of $p(w, t)$. Further numerical insights make evident that the small times used to check the GCFR (t smaller or equal to 3 mean free times) are far from the time where the asymptotic large deviation scaling starts working. In Fig. 11 indeed, we show the numerically obtained third cumulant of $\mathcal{W}(t)$ (rescaled by the first cumulant), as a function of time. The time of saturation is of the order of ~ 50 mean free times. The saturation value is in very good agreement with the value predicted by our theory, eq. (66). Note that this value is not at all trivial, since the third cumulant for a Gaussian distribution is zero. For this value of t, the numerically measured $\pi_t(w)$ is shown in Fig. 12, rescaled by $\langle w \rangle$. The accessible range of values from a numerical simulation is dramatically poor and it is already remarkable to have obtained a good measure of the third cumulant with such a resolution.

To understand the reason for a verification at small times of the GCFR we build upon an argument put forward in [15] where it was noted that for small arguments, π can be linearized, resulting in a linear behavior of $\pi_t(w) - \pi_t(-w)$. To go further and compute the prefactor of the linear term, we remark that near $w = 0$ the pdf of w is almost a

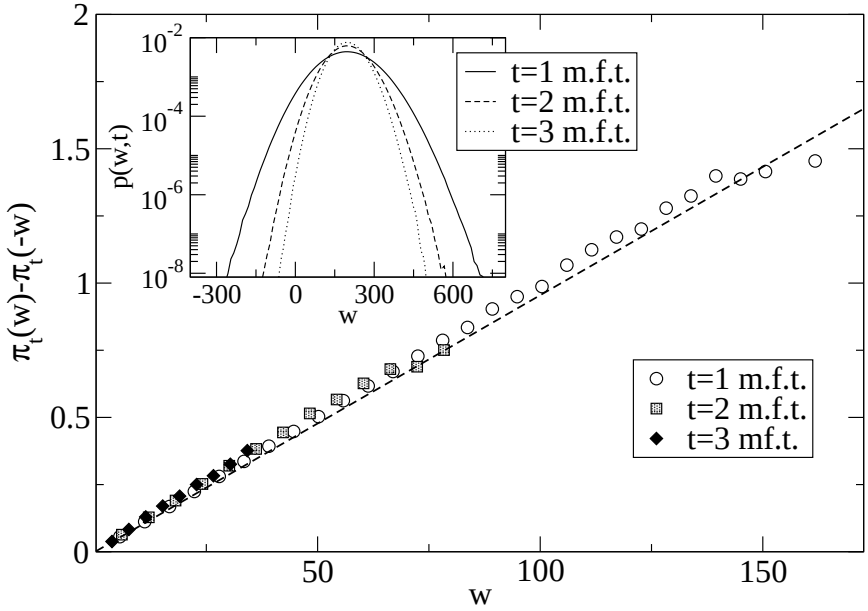

FIG. 10: Test of the Gallavotti-Cohen relation $\pi_t(w) - \pi_t(-w) = \beta_{eff} w$, for the system with $N = 100$ and $\Gamma = 0.5$ for different values of t. We recall that in this case $\langle w \rangle = 100$. The dashed line has slope $\beta = 1/T_g$. In the inset the corresponding $p(w, t)$ are shown.

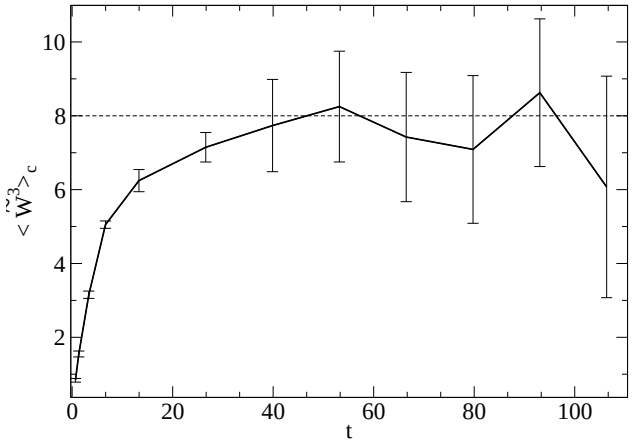

FIG. 11: Dimensionless third cumulant $\langle \tilde{\mathcal{W}}^3 \rangle_c = \langle \mathcal{W}^3 \rangle_c / (\langle \mathcal{W} \rangle T_g^2)$ for several times of integration. The time is in units of the mean collision time. Note that the time at which a stationary value of the rescaled cumulant is reached is much larger than the characteristic time of the system (the collision time). The horizontal dashed line shows the analytical prediction of Eq. (66): $\langle \widetilde{\mathcal{W}}^3 \rangle = 8$.

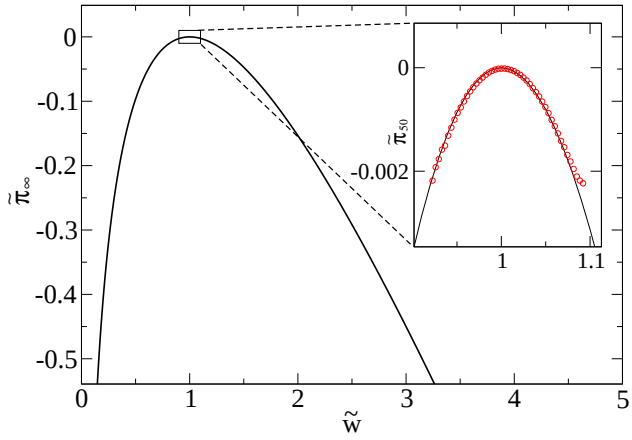

FIG. 12: Numerical measure of $\tilde{\pi}_t$ for a time of 50 collisions per particle (when a stationary value for the rescaled third cumulant is reached), shown with circles. The full line corresponds to $\pi_\infty(w)$ encoded in Eq. (68) and displayed in Fig. 3.

Gaussian. In the Gaussian case we immediately get $\pi_t(w) - \pi_t(-w) = \beta_{eff} w$ with $\beta_{eff} = 2\langle \mathcal{W}(t) \rangle / \langle \mathcal{W}(t)^2 \rangle_c$. The first two cumulants at small times are easily obtained considering an uncorrelated sequence of energy injection, obtaining $\langle \mathcal{W}(t) \rangle / t = N\Gamma d$ and $\langle \mathcal{W}(t)^2 \rangle_c / t = \langle (\sum_i \mathbf{F}_i^{th} \cdot \mathbf{v}_i)^2 \rangle_c = 2N\Gamma d T_g$. The value of the slope $\beta_{eff} = 1/T_g$ is a direct consequence of these simple relations. In this case the GCFR observed is the Green-Kubo-like (or Einstein) relation, which has been investigated numerically in [35] and analytically in [36], with the conclusion that such a relation holds within numerically accessible precision although it is, strictly speaking, invalid [36]. Small deviations from a Gaussian appear, in first approximation, as small deviations from the slope $1/T_g$, but the straight line behavior is robust since the first non-linear term of $\pi_t(w) - \pi_t(-w)$ is not w^2 but w^3.

B. Inelastic Maxwell Model

Numerical simulations of the Inelastic Maxwell Model have been performed with a Direct Simulation Monte Carlo analogous to the one used in the Hard Spheres model. Thanks to the simplifications present in this model, we are able to improve the number of collected data by a factor of more than ten. The distributions of the injected power $p(w,t)$ are shown in Fig. 13 for some choices of the restitution coefficient α. The driving amplitude Γ has been changed in order to keep constant the stationary granular temperature T_g. In Fig. 14 we have displayed the deviations from the Gaussian of $P(\mathcal{W},t)$. The non-Gaussianity of $P(\mathcal{W},t)$ is highly pronounced, but again it is striking only in the positive branch of the pdf. We have tried, with success, a fit with a fourth order polynomial. We observe that the reliability of such a fit increases with α, which is reminiscent of Sonine corrections phenomenology for the single particle velocity distribution alluded to earlier.

Finally, in Fig. 15, we have attempted a check of the Gallavotti-Cohen fluctuation relation. The relation seems to be systematically violated. This appears in two points: 1) the right-left ratio of the large deviation function is not a straight line; 2) the best fitting line has a slope which is larger than β. The "curvature"(and the deviation from the slope β) increases with decreasing values of α, indicating that the inelasticity is the cause of the deviation from the Gallavotti-Cohen relation. It should be noted that to achieve this result we have collected more than 4×10^{10} independent values of $\mathcal{W}(t)$, so that the statistics of the negative large deviations could be clearly displayed.

We also note that this numerically accessible violation of the GCFR is of a different nature than the one analytically shown in the previous sections since it occurs at the finite times, i.e. when π_t still displays negative w events.

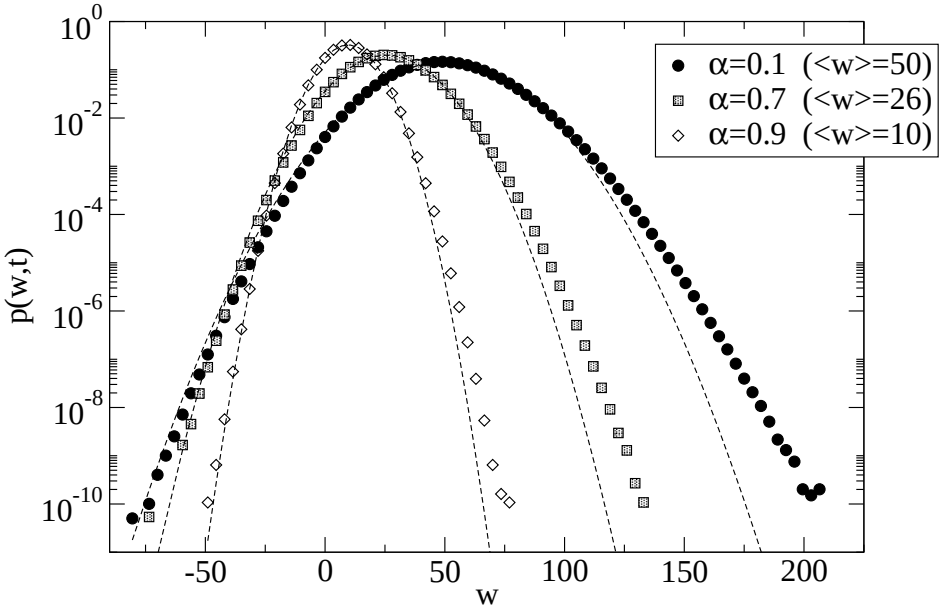

FIG. 13: $p(w,t) \equiv tP(wt,t)$ for different values of α (at fixed constant temperature T_g) in the Driven Inelastic Maxwell Model measured at a time t equal to 1 mean free time. The dashed lines are Gaussian distributions with the same mean and same variance. These distributions have been obtained with $\sim 4 \times 10^{10}$ independent values of $\mathcal{W}(t)$.

V. CONCLUSION

In this paper we have given the details of the derivation of an equation for the cumulants generating function $\mu(\lambda)$ of the injected power in granular gases, in the case of a homogeneous random driving mechanism. This equation appears as a generalization of the Boltzmann equation for the velocity pdf of the gas. It has also the remarkable physical interpretation of being the kinetic equation of a gas of annihilating/cloning/colliding particles with an external energy source. This interpretation leads to our main result: the large deviation function $\pi_\infty(w)$ of the injected power has no negative branch. We have also shown how to exploit a Sonine expansion to get better and better approximations of $\mu(\lambda)$ near $\lambda = 0$. We finally obtained $\mu(\lambda)$ in a closed analytical form by means of a generalized Gaussian hypothesis which is duly justified. This approximation becomes exact in the large dimension $d \to \infty$ limit. We have also

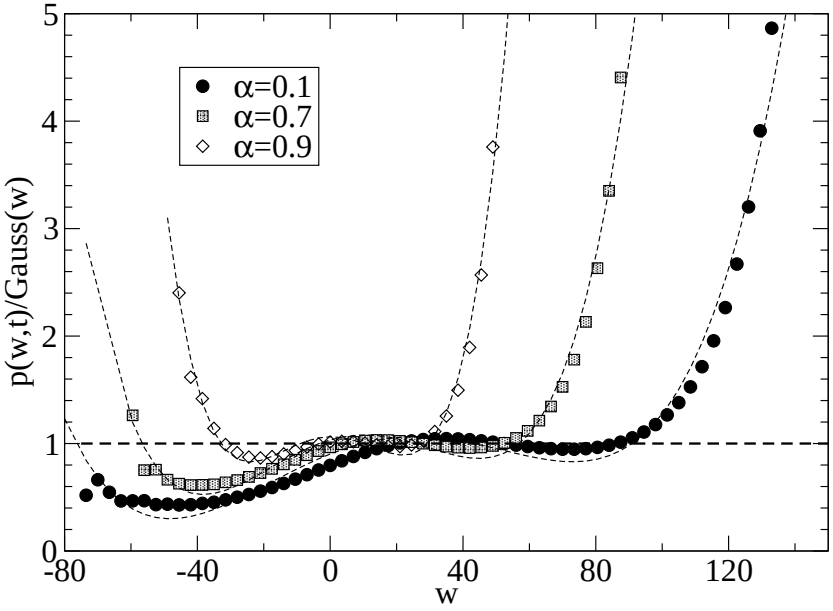

FIG. 14: $p(w,t)$ (at t equal to 1 mean free time) divided by a Gaussian with same average and same variance for different values of α (at fixed constant temperature T_g) in the Driven Inelastic Maxwell Model. The light dashed lines represent a fit with a polynomial of fourth order.

presented an argument that suggests the equivalence between the large deviation function of $\mathcal{W}(t)$ and that of the energy dissipated in collisions $\mathcal{D}(t)$. All these results are consistent with the absence of negative events in $\pi_\infty(w)$. This is at odds with previous studies that concluded that the GCFR could be satisfied for the integrated injected power in granular gases. Numerical simulations, on the other hand, show that the times at which a check of GCFR can be investigated are much smaller than the times required to reach the asymptotic large deviation scaling. At such small times the pdf of $\mathcal{W}(t)$ near $\mathcal{W}(t) = 0$ is almost Gaussian and this automatically leads to an artificial verification of the GCFR. On the other hand, the simulation of the inelastic Maxwell model instead of the inelastic Hard Spheres model made us able to gather much larger statistics so that we could see that even at finite times, for which $\pi_t(w)$ still displays negative events, the GC relation can be violated.

We emphasize here that observing non-Gaussian features in the tail of the distribution of injecting power does not guarantee that the asymptotic scaling regime has been reached. Non Gaussianities may equally well arise from short time effects, and it turns out that the latter mechanism is at work already at very short times. Observing an apparent GCFR at such short times appears to be an artifact, and much larger times are required to sample correctly the asymptotic regime. In this respect, the time behavior of rescaled cumulants (as displayed in Fig. 11) is a valuable tool to decide if the "transient" regime is over.

The analytical method put forward here to compute large temporal deviations is quite general and is particularly relevant in the context of the computation of probability distributions of global observables, which are useful, as underlined in the introduction, for the determination of universal features of non-equilibrium systems. For example, it applies to ballistically controlled processes, be they at equilibrium or not. Future work along these lines also includes the consideration of out of equilibrium granular gases without a steady state, such as freely cooling systems.

Acknowledgments

A. P. acknowledges the Marie Curie grant No. MEIF-CT-2003-500944. E.T. thanks the EC Human Potential program under contract HPRN-CT-2002-00307 (DYGLAGEMEN).

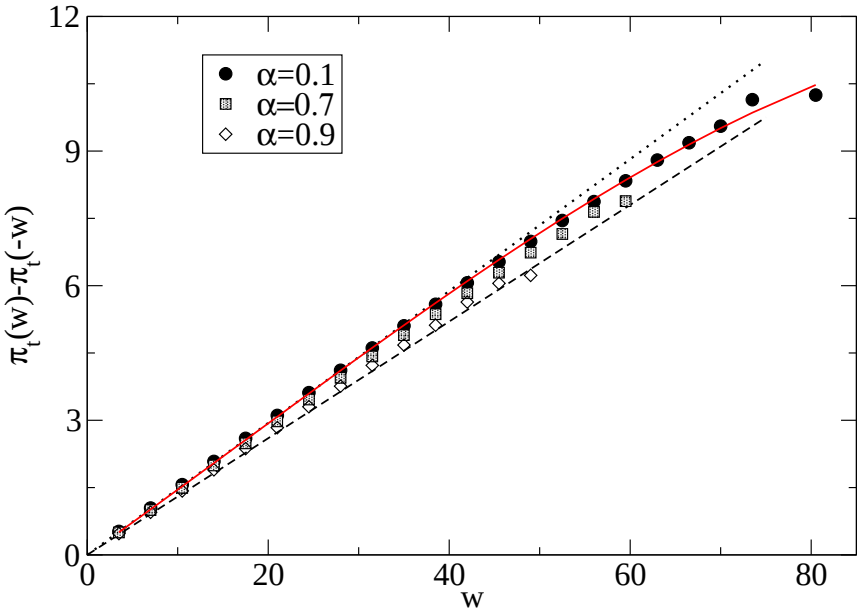

FIG. 15: (**Color online**). Finite time test of Gallavotti-Cohen relation for the injected power (with t equal to 1 mean free time), i.e. $\pi_t(w) - \pi_t(-w)$ vs. w, in a numerical simulation of the Driven Inelastic Maxwell Model with $N = 50$, and different values of α (the driving amplitude Γ has been rescaled in order to fix the granular temperature T_g). The dashed curve is a straight line with slope $\beta = 1/T_g$. The dotted curve is a straight line obtained fitting the $\alpha = 0.1$ data points until $w = 45$, useful as a guide for the eye. The thin (red) solid curve is a fit with a cubic $(0.28w + 5.6 \cdot 10^{-4}w^2 - 1.1 \cdot 10^{-5}w^3)$.

[1] N. van Kampen, *Stochastic processes in physics and chemistry*, North-Holland, 1992.
[2] A. Einstein, Ann. d. Phys. **17**, 549 (1905).
[3] L. Onsager, Phys. Rev. **37**, 405 (1931) ; Phys. Rev. **38**, 2265 (1931).
[4] M.S. Green, J. Chem. Phys. **22**, 398 (1954).
[5] R. Kubo, J. Phys. Soc. Japan **12**, 570 (1957).
[6] S. R. de Groot and P. Mazur, *Non-equilibrium thermodynamics*, North-Holland, 1969.
[7] S.T. Bramwell, P.C.W. Holdsworth and J.-F. Pinton, Nature **396**, 552-554, (1998).
[8] J. Javier Brey, M. I. García de Soria, P. Maynar, and M. J. Ruiz-Montero, Phys. Rev. Lett. **94**, 098001 (2005)
[9] D.J. Evans, E.G.D. Cohen and G.P. Morriss, Phys. Rev. Lett. **71**, 2401 (1993).
[10] G. Gallavotti and E.G.D. Cohen, Phys. Rev. Lett. **74**, 2694 (1995).
[11] D. J. Evans and G.P. Morriss, *Statistical Mechanics of Nonequilibrium Liquids*, Academic Press, London, 1990; G. P. Morriss and C. P. Dettmann, Chaos **8**, 321 (1998).
[12] J. Kurchan, J. Phys. A **31**, 3719 (1998).
[13] J.L. Lebowitz and H. Spohn, J. Stat. Phys. **95**, 333 (1999).
[14] S. Ciliberto, and C. Laroche, Journal de Physique IV, **8** , 215 (1998); N. Garnier and S. Ciliberto, Phys. Rev. E **71** 060101(R) (2005); S. Ciliberto, N. Garnier, S. Hernandez, C. Lacpatia, J.-F. Pinton and G. Ruiz Chavarria, Physica A **340** (1-3) pp 240-250 (2004).
[15] S. Aumaître, S. Fauve, S. McNamara and P. Poggi, Eur. Phys. J. B **19**, 449 (2001).
[16] J. Farago, J. Stat. Phys. **107**, 781 (2002).
[17] K. Feitosa and N. Menon, Phys. Rev. Lett. **92**, 164301 (2004).
[18] P. Visco, A. Puglisi, A. Barrat, E. Trizac and F. van Wijland, accepted in Europhysics Letters (2005).
[19] A. Puglisi, P. Visco, A. Barrat, E. Trizac and F. van Wijland, submitted (2005).
[20] D. R. M. Williams and F. C. MacKintosh, Phys. Rev. E **54** R9 (1996); G. Peng and T. Ohta, Phys. Rev. E **58**, 4737 (1998); T.P.C. van Noije, M.H. Ernst, E. Trizac and I. Pagonabarraga, Phys. Rev E **59**, 4326 (1999); C. Henrique, G. Batrouni and D. Bideau, Phys. Rev. E **63**, 011304 (2000); S. J. Moon, M. D. Shattuck and J. B. Swift, Phys. Rev. E **64**, 031303 (2001); I. Pagonabarraga, E. Trizac, T.P.C. van Noije and M.H. Ernst, Phys. Rev. E **65**, 011303 (2002).
[21] A. Prevost, D.A. Egolf, and J.S. Urbach, Phys. Rev. Lett. **89**, 084301 (2002).
[22] T.P.C. van Noije and M.H. Ernst, Granular Matter **1**, 57 (1998).
[23] J.M. Montanero and A. Santos, Granular Matter **2**, 53 (2000).
[24] F. Coppex, M. Droz, J. Piasecki and E. Trizac, Physica A **329**, 114 (2003).

[25] G. A. Bird, Molecular Gas Dynamics and the Direct Simulation of Gas Flows, Clarendon 1994 (Oxford).
[26] J. Farago, Physica A **331**, 69 (2004).
[27] R. van Zon and E. G. D. Cohen, Phys. Rev. Lett. **91**, 110601 (2003).
[28] W. Feller, *An Introduction to Probability Theory and Its Applications*, John Wiley & Sons 1966.
[29] J. C. Maxwell, Phil. Trans. **157**, 49 (1867).
[30] A. Baldassarri, U. Marini Bettolo Marconi and A. Puglisi, Europhys. Lett. **58**, 14-20 (2002).
[31] E. Ben-Naim and P.L. Krapivsky, J. Phys. A **35**, L147 (2002); Lecture Notes in Physics **624**, 65 (2003).
[32] M. H. Ernst and R. Brito, Europhys. Lett. **58**, 182 (2002).
[33] A. V. Bobylev, J. A. Carrillo, I. M. Gamba, J. Stat. Phys. **98**, 743 (2000).
[34] A. Santos, Physica A **321**, 442 (2003).
[35] A. Puglisi, A. Baldassarri and V. Loreto, Phys. Rev. E **66**, 061305 (2002).
[36] V. Garzó, Physica A **343**, 105 (2004).